Eur. Phys. J. C (2020) 80:450
https://doi.org/10.1140/epjc/s10052-020-7997-4

THE EUROPEAN PHYSICAL JOURNAL C

Regular Article - Experimental Physics

Search for light long-lived neutral particles produced in pp collisions at $\sqrt{s} = 13$ TeV and decaying into collimated leptons or light hadrons with the ATLAS detector

ATLAS Collaboration[*]

CERN, 1211 Geneva 23, Switzerland

Received: 4 September 2019 / Accepted: 4 May 2020 / Published online: 20 May 2020

Abstract Several models of physics beyond the Standard Model predict the existence of dark photons, light neutral particles decaying into collimated leptons or light hadrons. This paper presents a search for long-lived dark photons produced from the decay of a Higgs boson or a heavy scalar boson and decaying into displaced collimated Standard Model fermions. The search uses data corresponding to an integrated luminosity of 36.1 fb^{-1} collected in proton–proton collisions at $\sqrt{s} = 13$ TeV recorded in 2015–2016 with the ATLAS detector at the Large Hadron Collider. The observed number of events is consistent with the expected background, and limits on the production cross section times branching fraction as a function of the proper decay length of the dark photon are reported. A cross section times branching fraction above 4 pb is excluded for a Higgs boson decaying into two dark photons for dark-photon decay lengths between 1.5 mm and 307 mm.

1 Introduction

Several extensions of the Standard Model (SM) predict the existence of a dark sector weakly coupled to the SM [1–4]. Depending on the structure of the dark sector and its coupling to the SM, some unstable dark states may be produced at colliders, and could decay into SM particles with sizeable branching fractions. In order to avoid a new long-range force, a dark Higgs boson is introduced in such scenarios, to give mass to the dark gauge bosons. The dark Higgs boson may also lead to an exotic decay mode of the Higgs boson, via mixing between the two Higgs sectors, which is one of the favoured production modes that may be probed at the Large Hadron Collider (LHC). This is the mode explored in this search. Branching fractions of up to 10% are currently not excluded for Higgs-boson decays into exotic final states [5,6]. This paper investigates the case where the two sectors couple via a vector portal, in which a dark photon (γ_d) mixes kinetically with the SM photon and decays into SM leptons and light quarks [7–9]. The kinetic mixing term (ϵ), which can vary over a wide range of values, $\epsilon \sim 10^{-11}$–10^{-2}, determines the lifetime of the dark photon. For a small kinetic mixing value, the γ_d has a long lifetime, so that it decays at a macroscopic distance from its production point. This analysis focuses on small values of the kinetic mixing term, $\epsilon < 10^{-5}$, and a dark photon mass range between twice the muon mass and twice the tau mass. Due to their small mass, the dark photons are expected to be produced with large boosts, resulting in collimated groups of leptons and light hadrons in a jet-like structure, referred to hereafter as dark-photon jets (DPJs).

The search for displaced DPJs presented in this paper uses the dataset collected by the ATLAS detector during 2015–2016 in proton–proton (pp) collisions at a centre-of-mass energy $\sqrt{s} = 13$ TeV, corresponding to an integrated luminosity of 36.1 fb^{-1}. The analysis exploits multivariate techniques for the suppression of the main multi-jet background, optimised for the different DPJ channels. This technique allows the exploitation of the fully hadronic signature for the first time in ATLAS DPJ searches, resulting in increased sensitivity compared with previous ATLAS results using the data collected in 2011 and 2012 at 7 and 8 TeV respectively [10,11]. The results are complementary to those from related ATLAS searches for prompt DPJs using 7 and 8 TeV data [12–14], which probed higher values of ϵ, and for displaced dimuon vertices using 13 TeV data [15], which probed higher dark photon mass values. Related searches for dark photons were conducted by the CDF and D0 collaborations at the Tevatron [16–18] and by the CMS [19–22] and LHCb [23,24] collaborations at the LHC. Additional constraints on scenarios with dark photons are extracted from, e.g., beam-dump and fixed-target experiments [25–35], e^+e^- colliders [36–44], electron and muon anomalous magnetic moment measurements [45–47] and astrophysical observations [48,49]. Given the various constraints, a displaced dark

[*] e-mail: atlas.publications@cern.ch

photon with a kinetic mixing term $\epsilon < 10^{-5}$ is allowed for γ_d masses greater than 100 MeV.

2 The ATLAS detector

ATLAS [50] is a multipurpose detector at the LHC, consisting of an inner detector (ID) contained in a superconducting solenoid, which provides a 2 T magnetic field parallel to the beam direction, electromagnetic and hadronic calorimeters (ECAL and HCAL) and a muon spectrometer (MS) that has a system of three large air-core toroid magnets, each composed of eight coils.

The ID provides measurements of charged-particle momenta in the region of pseudorapidity $|\eta| \leq 2.5$.[1] The highest spatial resolution is obtained around the vertex region using semiconductor pixel detectors arranged in four barrel layers [51,52] at average radii of 3.3 cm, 5.05 cm, 8.85 cm, and 12.25 cm, and three discs on each side, covering radii between 9 and 15 cm. The pixel detector is surrounded by four layers of silicon microstrips covering radial distances from 29.9 to 56.0 cm. These silicon detectors are complemented by a transition radiation tracker (TRT) covering radial distances from 56.3 to 106.6 cm.

The ECAL and HCAL calorimeter system covers $|\eta| \leq 4.9$, and has a total depth of 9.7 interaction lengths at $\eta = 0$, including 22 radiation lengths in the ECAL. The ECAL barrel starts at a radius of 1.41 m and ends at 1.96 m with a z extension of ± 3.21 m, covering the $|\eta| \leq 1.475$ interval. In the $1.37 \leq |\eta| \leq 3.2$ region, the ECAL endcap starts at $z \pm 3.70$ m and end at $z \pm 4.25$ m. The HCAL barrel starts at a radius of 2.28 m and ends at 4.25 m with a z extension of ± 4.10 m, covering the $|\eta| \leq 1.0$ interval. In the endcaps regions up to $|\eta| \leq 4.9$, the HCAL starts at $z \pm 4.3$ m and ends at $z \pm 6.05$ m.

The MS provides trigger information and momentum measurements for charged particles in the pseudorapidity ranges $|\eta| \leq 2.4$ and $|\eta| \leq 2.7$ respectively. It consists of one barrel ($|\eta| \leq 1.05$) and two endcaps ($1.05 \leq |\eta| \leq 2.7$), each with 16 sectors in ϕ, equipped with fast detectors for triggering and with chambers for reconstructing the tracks of the outgoing muons with high spatial precision. The MS detectors are arranged in three stations at increasing distances from the IP: inner, middle and outer. Three planes of MS trigger chambers are located in the middle and outer stations. The toroidal magnetic field allows precise reconstruction of charged-particle momenta independent of the ID information.

The ATLAS trigger system has two levels [53], level-1 (L1) and the high-level trigger (HLT). The L1 trigger is a hardware-based system using information from the calorimeters and MS. It defines one or more regions-of-interest (RoI), which are geometric regions of the detector identified by (η, ϕ) coordinates, containing interesting physics objects. The L1 trigger reduces the event rate from the LHC crossing frequency of 40 MHz to a design value of 100 kHz. L1 RoI information provides a seed for the reconstruction of physics objects by the HLT, a software-based system that can access information from all subdetectors. It is implemented in software running on a PC farm that processes the events and reduces the rate of recorded events to 1 kHz.

3 Benchmark model

Among the numerous models predicting dark photons, one class particularly interesting for the LHC features a hidden sector communicating with the SM through the Higgs portal for production and through vector portal for decay. The benchmark model used in this analysis is the Falkowski–Ruderman–Volansky–Zupan (FRVZ) model [8,9], where a pair of dark fermions f_{d_2} is produced via a Higgs boson (H) decay. Two different cases of this model are considered, involving the production of either two or four dark photons. In the first case, shown in Fig. 1 (left), each dark fermion decays into a γ_d and a lighter dark fermion assumed to be the hidden lightest stable particle (HLSP). In the second case, shown in Fig. 1 (right), each dark fermion decays into an

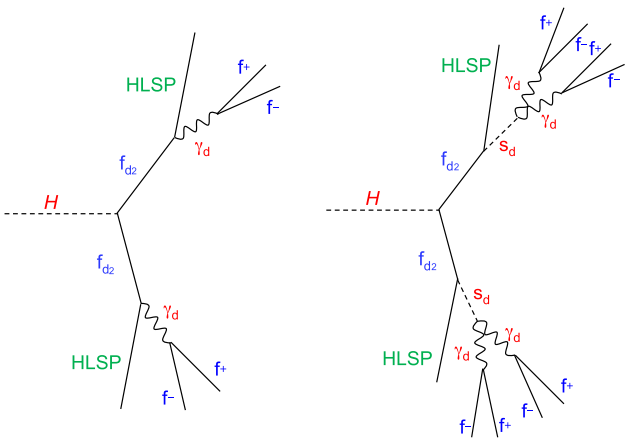

Fig. 1 The two processes of the FRVZ model used as benchmarks in the analysis. In the first process (left), the dark fermion f_{d_2} decays into a γ_d and an HLSP. In the second process (right), the dark fermion f_{d_2} decays into an HLSP and a dark scalar s_d that in turn decays into a pair of dark photons. The γ_d decays into SM fermions, denoted by f^+ and f^-

[1] ATLAS uses a right-handed coordinate system with its origin at the nominal interaction point in the centre of the detector and the z-axis coinciding with the beam-pipe axis. The x-axis points from the interaction point to the centre of the LHC ring, and the y-axis points upward. Cylindrical coordinates (r,ϕ) are used in the transverse plane, ϕ being the azimuthal angle around the beam pipe. The pseudorapidity is defined in terms of the polar angle θ as $\eta = -\ln \tan(\theta/2)$.

Table 1 Parameters used for the Monte Carlo simulations of the benchmark model

Sample	m_H (GeV)	$m_{f_{d_2}}$ (GeV)	m_{HLSP} (GeV)	m_{s_d} (GeV)	m_{γ_d} (GeV)	$c\tau$ (mm)
$H \to 2\gamma_d + X$	125	5.0	2.0	–	0.4	49.23
$H \to 4\gamma_d + X$	125	5.0	2.0	2.0	0.4	82.40
$H \to 2\gamma_d + X$	800	5.0	2.0	–	0.4	11.76
$H \to 4\gamma_d + X$	800	5.0	2.0	2.0	0.4	21.04

HLSP and a dark scalar s_d that in turn decays into a pair of dark photons.

In general, dark-sector radiation [54] can produce extra dark photons. The number of radiated dark photons is proportional to the size of the dark gauge coupling α_d [7]. The dark radiation is not considered in this signal model, which corresponds to an assumed dark coupling $\alpha_d \lesssim 0.01$.

The vector portal communication of the hidden sector with the SM is through kinetic mixing of the dark photon and the standard photon

$$\mathcal{L}_{\text{gauge mixing}} = \frac{\epsilon}{2} B_{\mu\nu} b^{\mu\nu},$$

where $B_{\mu\nu}$ and $b_{\mu\nu}$ denote the field strengths of the electromagnetic fields for the SM and dark sector respectively, and ϵ is the kinetic mixing parameter. A dark photon with a mass m_{γ_d} up to a few GeV that mixes kinetically with the SM photon will decay into leptons or light mesons, with branching fractions that depend on its mass [8,55,56].

The mean lifetime τ, expressed in seconds, of the γ_d is related to the kinetic mixing parameter [57] by the relation

$$\tau \propto \left(\frac{10^{-4}}{\epsilon}\right)^2 \left(\frac{100\ \text{MeV}}{m_{\gamma_d}}\right). \quad (1)$$

Equation (1) is an approximate expression based on the full relation in Ref. [56].

4 Data and simulation samples

The analysis presented in this paper uses $\sqrt{s} = 13$ TeV pp collision data recorded by the ATLAS detector during the 2015–2016 data-taking periods. Only runs in which all the ATLAS subdetectors were operating normally are selected. The total integrated luminosities are 3.2 fb^{-1} and 32.9 fb^{-1} for 2015 and 2016 respectively.

Data were collected using a set of dedicated triggers that were active during collision bunch crossings as well as during empty and unpaired bunch-crossing slots. The LHC configuration for pp collisions contains 3564 bunch-crossing slots per revolution. An empty bunch-crossing is defined as a slot in which neither beam is filled with protons, and in addition is separated from filled bunches by at least five unfilled bunches on each side. Data collected during empty bunch crossings, referred to as the cosmic dataset, are used for the estimation of the cosmic-ray background. The ratio of the number of filled to empty bunch crossings, $F_{\text{CR}} = 2.1$, is used to scale the number of events in the cosmic dataset to that in the pp collision data. In unpaired bunch crossings, protons are present in only one of the two beams. Data taken during unpaired bunch crossings are used to study characteristic features of beam-induced backgrounds [58] (BIB) and are referred to as the BIB dataset.

Monte Carlo (MC) simulation samples were produced for the model considered in this paper and are summarised in Table 1.

Samples were generated for the Higgs boson mass of 125 GeV, and for a hypothetical beyond-the-SM (BSM) heavy scalar boson with a mass of 800 GeV, considering only the dominant gluon–gluon fusion (ggF) production mechanism. The ggF Higgs boson production cross section in pp collisions at $\sqrt{s} = 13$ TeV, estimated at next-to-next-to-leading order (NNLO) [59–62], is $\sigma_{\text{SM}} = 43.87$ pb for $m_H = 125$ GeV. The BSM heavy scalar with a mass of 800 GeV production cross section is conventionally assumed to be $\sigma = 5$ pb.

The mass of the hidden fermion $m_{f_{d_2}}$ and of the hidden scalar m_{s_d} were chosen to be low relative to the Higgs boson mass. Due to the production from a two-body decay of the Higgs boson generated at rest in the transverse plane, events with two back-to-back DPJs are expected. This is also the case leading to four dark photons where each DPJ consist of two collimated dark photons.

The dark-photon mass was chosen to be 0.4 GeV, above the pion pair mass threshold, and the γ_d decay branching fractions ($\mathcal{B}$) are expected to be $\mathcal{B}(\gamma_d \to ee) = 45\%$, $\mathcal{B}(\gamma_d \to \mu\mu) = 45\%$, $\mathcal{B}(\gamma_d \to \pi\pi) = 10\%$ [8]. In the generated samples, the proper decay length $c\tau$ of the γ_d was chosen such that $\sim 80\%$ of the decays occur in the volume delimited by the muon trigger chambers (i.e. up to 7 m in radius and 13 m along the z-axis). Since the analysis is sensitive to a wide range of mean proper lifetimes, a weighting method is used to extrapolate the signal efficiency to other mean proper lifetimes.

All MC samples described above were generated at leading order using MadGraph 5_aMC@NLO 2.2.3 [63] interfaced to Pythia 8.210 [64] for parton shower generation. The A14 set of tuned parameters (tune) for parton showering and hadronisation [65] was used together with the NNPDF2.3LO parton distribution function (PDF) set [66].

One of the main SM backgrounds in this analysis is multi-jet events. Such events were simulated to perform background studies and to evaluate systematic uncertainties. The MC samples were generated with Pythia 8.210 using the same tune and PDF as for the signal samples.

Potential sources of background also include W+jets, Z+jets, $t\bar{t}$, single-top-quark, WW, WZ, and ZZ events. Simulation samples are used to study these backgrounds. The W+jets, Z+jets , WW, WZ, and ZZ events were generated using Sherpa 2.2.2 [67] with the NNPDF 3.0 NNLO [68] PDF set. Single-top-quark and $t\bar{t}$ MC samples were generated using Powheg- box 1.2856 [69–72] and Pythia 6.428 [73] with the Perugia2012 [74] tune for parton showering and hadronisation, and CT10/CTEQ6L1 [75,76] PDF sets.

Data and MC samples of $J/\psi \to \mu\mu$ events are used to evaluate systematic uncertainties in muon trigger and reconstruction efficiencies. The MC sample was generated using Pythia8+Photos++ [77] with the A14 tune for parton showering and hadronisation, and the CTEQ6L1 PDF set. The $J/\psi \to \mu\mu$ data sample was selected in 2015–2016 pp collisions using the triggers described in Ref. [78].

The generated MC events were processed through a full simulation of the ATLAS detector geometry and response [79] using the Geant4 [80] toolkit. The simulation included multiple pp interactions per bunch crossing (pile-up), as well as the detector response to interactions in bunch crossings before and after the one producing the hard interaction. To model the effect of pile-up, simulated inelastic pp events were overlaid on each generated signal and background event. The multiple interactions were simulated with Pythia 8.210 using the A2 tune [81] and the MSTW2008LO PDF set [82].

5 Definition of the dark-photon jets

5.1 Dark-photon jet classification

Displaced DPJs are reconstructed with criteria that depend on the γ_d decay channel. A γ_d decaying into a muon pair is searched for by looking for two closely spaced muon tracks in the MS, while a γ_d decaying into an electron or pion pair, given the high boost of the γ_d, is searched for as an energy deposit in the calorimeters identified as a single narrow jet. MC simulations show that DPJs containing two dark photons both decaying into an electron or pion pair are reconstructed as a single jet.

Tracks that are reconstructed in the MS and are not matched to any track in the ID are used to identify displaced γ_d decays into muons. Since the ID track reconstruction in ATLAS [83] requires at least one hit in one of the two innermost pixel layers, this analysis is sensitive only to displaced γ_d decays occurring after the first pixel layers. The search is limited to the pseudorapidity interval $|\eta| < 2.5$, corresponding to the ID coverage, to ensure that selected muons are isolated from ID tracks. Muons with pseudorapidity in the range $1.0 \leq |\eta| \leq 1.1$ are rejected to avoid the transition region of the MS between barrel and endcap. In order to reconstruct γ_d decays that occur outside of the innermost layer of muon chambers but before the first MS trigger chamber, muons are required to have at least one hit in two of the three MS tracking station.

Jets used in this search are reconstructed from clusters [84] of energy deposits in the ECAL and HCAL using the anti-k_t algorithm [85,86] with radius parameter $R = 0.4$. The search is limited to γ_d decays into electron or hadron pairs in the hadronic calorimeter. Jets produced in the HCAL are expected to be isolated from activity in the ID, with a high ratio of energy deposited in the HCAL (E_{HCAL}) to energy deposited in the ECAL (E_{ECAL}), and appear narrower than ordinary jets. The standard jet-cleaning requirements [87] applied in most ATLAS analyses reject jets with high values of $E_{\mathrm{HCAL}}/E_{\mathrm{ECAL}}$. A dedicated cleaning algorithm for jets created in the HCAL is applied instead, with no requirements on the ratio $E_{\mathrm{HCAL}}/E_{\mathrm{ECAL}}$. Jets are required to have transverse momentum $p_{\mathrm{T}} \geq 20$ GeV and $|\eta| < 2.5$. In addition, the weighted time of the energy deposit in the calorimeter cells is required to be in the range [–4 ns, 4 ns] of the expected arrival time for particles produced at $t = 0$ (bunch-crossing time) and moving with the speed of light, to reduce cosmic-ray background and BIB jets.

DPJs are classified according to the number of muons and jets found within a given cone of angular size $\Delta R \equiv \sqrt{(\Delta\phi)^2 + (\Delta\eta)^2}$ around a muon or jet candidate with the highest transverse momentum. The cone size is fixed to $\Delta R = 0.4$, since the MC simulations show that this selection retains up to 90% of the dark-photon decay products in the $H \to 4\gamma_d + X$ decay channel with $m_H = 125$ GeV. The DPJ classification is summarised as follows:

- **muonic-DPJ (μDPJ)** – to select DPJs with all constituent dark photons decaying into muons, at least two muons are required and no jets are allowed in the cone.
- **hadronic-DPJ (hDPJ)** – to select DPJs with all constituent dark photons decaying into electron or pion pairs in the HCAL, one jet is required and no muons are allowed to be in the cone. The electromagnetic fraction of the jet energy, defined as the ratio of the energy deposited

in the ECAL to the total jet energy ($E_{\mathrm{ECAL}}/E_{\mathrm{total}}$), is required to be less than 0.4. This helps reduce the overwhelming background due to multi-jet production. This variable is also used later, as described in Sect. 5.3

Reconstructed DPJs with both muon and jet constituents are not considered in this analysis.

5.2 Muonic-DPJ selection

Muonic-DPJs are reconstructed using a Cambridge–Aachen clustering algorithm [88] that combines all the muons lying within a cone of fixed size in (η, ϕ) space. The algorithm starts from the highest-p_{T} muon, searching for additional muons within the $\Delta R = 0.4$ cone around the muon momentum vector. If a second muon is found in the cone, the axis of the cone is rotated to the vector sum of the momenta of the two muons, and the search is repeated until no additional muons are found in the cone.

Cosmic-ray muons that cross the detector in time coincidence with a pp interaction constitute the main source of background to the muonic-DPJ. The cosmic dataset is used to study this background. A boosted decision tree (BDT) with gradient boosting, implemented in the TMVA framework [89], is trained to discriminate signal DPJs from the DPJ candidates that originate from cosmic-ray background. The BDT uses the following track variables, for each muon in the DPJ, to classify a DPJ as being from signal or background:

- longitudinal impact parameter z_0, defined as the minimum separation in the z-coordinate between the muon track and the primary vertex (PV);[2]
- arrival times measured by the trigger detectors of the MS;
- pseudorapidity η;
- azimuthal angle ϕ.

Even if the decay is displaced, signal muons point to the primary vertex because of the high boost of the dark photon, resulting in a narrow z_0 distribution peaking around zero. By contrast, cosmic-ray muons have a broad z_0 distribution.

Cosmic-ray muons mainly come through the two shafts above the ATLAS detector, resulting in two well-defined peaks in the η and ϕ distributions. Each hit in the trigger detector of the MS provides a measurement of the time for the muon track, corrected by the time of flight assuming the pp interaction point as the origin of the muon [90]. The difference in time measured by the two layers in the middle station and in the outer station is thus useful for discriminating between cosmic-ray muons and collision muons. Since cosmic-ray muons are downward going, their arrival times in the layers in the upper part of the MS ($0 < \phi < \pi$) are different from those of collision muons, which are upward-going in this part of the detector. In the lower part of the MS ($\pi < \phi < 2\pi$), cosmic-ray muons and collision muons travel downwards, making hit timing less useful for separating between them.

The cosmic dataset and the signal MC sample $H \to 2\gamma_{\mathrm{d}} + X$ with $m_H = 125$ GeV are used for the training of the BDT. The gain in signal significance obtained from dedicated BDT training with the other signal MC samples is found to be negligible. Figure 2 (left) shows the BDT output (μBDT) for the constituent muons of the μDPJs: the distribution provides a clear separation between signal and background muons from cosmic rays. The μBDT output is required to be $\mu\mathrm{BDT} > 0.21$; the value is chosen to yield the highest signal significance, $S/\sqrt{S+B}$, where S is the number of signal events and B the number of background events.

5.3 Hadronic-DPJ selection

Signal jets are discriminated from multi-jets using a second classifier also based on a BDT (hBDT). The following variables are used as input to the hBDT:

- jet width, defined as the p_{T}-weighted sum of the ΔR between each energy cluster and the jet axis;
- jet vertex tagger (JVT) output [91];
- $E_{\mathrm{ECAL}}/E_{\mathrm{total}}$;
- jet mass, as defined by the jet clustering algorithm [92];
- jet charge, defined as the momentum-weighted charge sum constructed from tracks associated with the jet; tracks are associated with jets using ghost association [93];
- jet timing, defined as the energy-weighted average of the timing for each cell in the jet.

The JVT is designed to differentiate between pile-up jets and jets originating from the PV. The algorithm uses a multivariate combination of track variables that are sensitive to pile-up. Since jets produced in the hadronic calorimeter have a JVT output distribution similar to that of pile-up jets, the JVT output is used for selection of hadronic-DPJs. Possible pile-up jets contamination is reduced by the analysis selection to a negligible level.

The signal MC sample $H \to 2\gamma_{\mathrm{d}} + X$ with $m_H = 125$ GeV and the simulated multi-jet background events are used for the BDT training. The gain in signal significance obtained from dedicated BDT training with the other signal MC samples is found to be negligible. Figure 2 (right) shows the BDT output for the hDPJs (hBDT). The peak at ~ -0.2 in the BDT

[2] The primary interaction vertex is defined to be the vertex with the largest value of Σp_{T}^2, the sum of the squared transverse momenta of all the tracks originating from the vertex.

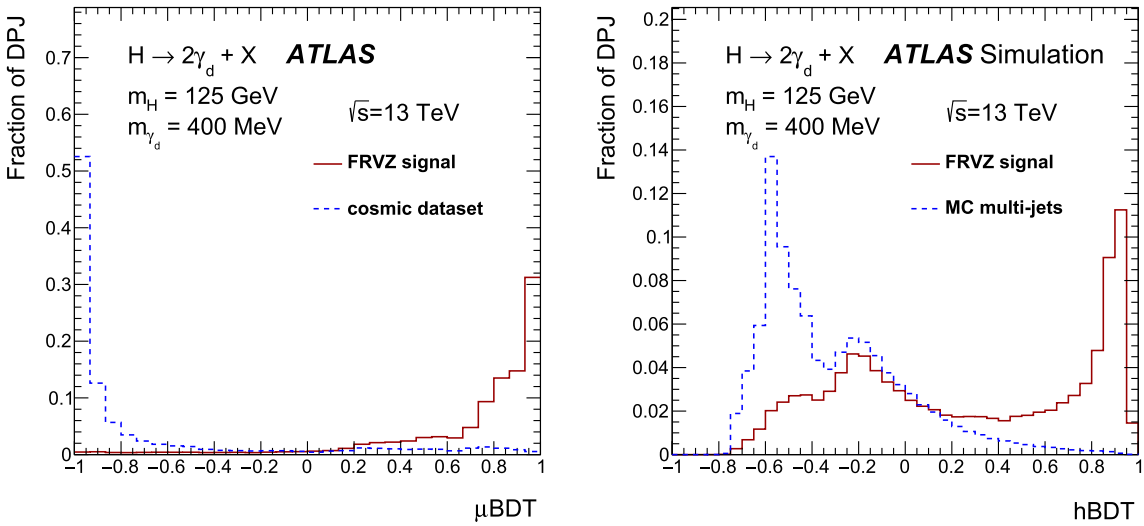

Fig. 2 BDT output distributions for signal and background for μDPJs (left) and hDPJs (right). For muonic-DPJs the background is the cosmic dataset and the FRVZ signal sample is the $H \rightarrow 2\gamma_{\mathrm{d}} + X$ process with $m_H = 125$ GeV. For hadronic-DPJs the signal MC sample is the $H \rightarrow 2\gamma_{\mathrm{d}} + X$ process with $m_H = 125$ GeV and the background is the simulated multi-jet background sample

distributions corresponds to jets with a JVT output that indicates a low pile-up probability. The hBDT output is required to be hBDT > 0.91; the value is chosen to yield the highest signal significance.

6 Trigger and event selection

The standard ATLAS triggers are optimised to select prompt events and are thus usually very inefficient in the selection of displaced objects. This search uses events selected by the logical OR of three dedicated triggers targeting displaced objects: two muon triggers and one calorimeter trigger.

The L1 muon trigger used in this analysis requires hits in the middle stations to create a low-p_{T} (≥ 6 GeV) muon RoI or hits in both the middle and outer stations for a high-p_{T} (≥ 20 GeV) muon RoI. The muon RoIs have a $\Delta\eta \times \Delta\phi$ spatial extent of 0.2×0.2 in the barrel and of 0.1×0.1 in the endcaps. L1 RoI information seeds the reconstruction of muon momenta by the HLT, which uses precision-chamber information to confirm or reject the L1 decision.

The first muon trigger, the tri-muon MS-only [94], requires at least three L1 muons with $p_{\mathrm{T}} \geq 6$ GeV in the event, confirmed by the HLT using only MS information.

The second muon trigger, the muon narrow-scan, is specifically designed to select non-prompt collimated muons originating in the region between the first pixel layer and the first muon trigger plane. It requires an L1 muon with $p_{\mathrm{T}} \geq 20$ GeV confirmed by the HLT using only MS information. At the HLT a 'scan' is then performed in a cone of $\Delta R = 0.5$ around this muon, looking for a second muon reconstructed using only MS information. During the course of the 2015–2016 data taking, in order to stay within the allocated trigger-rate limits given the increasing luminosity delivered by the LHC, the p_{T} requirement on the second muon was increased from 6 GeV to 15 GeV. In addition, both muons were required to be unmatched to any track in the ID, and isolation was required for the leading muon.[3] This tends to selects events with dark photons of higher p_{T} and with more displaced decay position.

The calorimeter trigger, the CalRatio [94], is designed to select narrow jets produced in the hadronic calorimeter. At L1, the trigger requires a transverse-energy deposit of $E_{\mathrm{T}} \geq 60$ GeV within a 0.2×0.2 ($\Delta\eta \times \Delta\phi$) region in the pseudorapidity range $|\eta| \leq 2.4$. At the HLT, jet reconstruction is then performed with the anti-k_t algorithm using a radius parameter of $R = 0.4$. Transverse energy $E_{\mathrm{T}} \geq 30$ GeV and $\log(E_{\mathrm{HCAL}}/E_{\mathrm{ECAL}}) \geq 1.2$ are required. Jets are required to have no tracks with $p_{\mathrm{T}} \geq 2$ GeV within $\Delta R = 0.2$ of the jet axis. Finally, jets are required to pass a BIB removal algorithm that relies on calorimeter cell timing and position. Muons from BIB enter the HCAL and can radiate a bremsstrahlung photon, generating an energy deposit that may be reconstructed as a jet with characteristics similar to the hadronic-DPJ. The algorithm identifies events as containing BIB if the triggering jet has at least four HCAL cells at the same ϕ and in the same layer with timing consistent with that of a BIB energy deposit.

Two DPJs satisfying the selection criteria described in Sect. 5 are required in the events selected by the triggers. If more than two DPJs are reconstructed, the one with the

[3] The isolation is quantified by summing the p_{T} of inner detector tracks with $p_{\mathrm{T}} > 1$ GeV, excluding the muon candidate, which are found in a cone of $\Delta R = 0.2$ around the muon candidate.

Table 2 Summary of the definitions of the signal regions (SRs) and validation regions (VRs) used in the ABCD method

Region	Channel	Criteria
SR	μDPJ–μDPJ	μBDT > 0.21 for both DPJs
	μDPJ–hDPJ	μBDT > 0.21 and hBDT > 0.91
	hDPJ–hDPJ	hBDT > 0.91 for both DPJs
VR	μDPJ–μDPJ	$-0.75 <$ μBDT < 0.35 for leading μDPJ, μBDT > -0.7 for subleading μDPJ
	μDPJ–hDPJ	$-0.5 <$ μBDT < 0.8 and $0.2 <$ hBDT < 0.8
	hDPJ–hDPJ	hBDT < 0.91 for both DPJs

highest transverse momentum, labelled the leading DPJ, and the one farthest in $\Delta\phi$ from the leading one, labelled the subleading DPJ, are used to classify the event. More than two DPJs are found in 9% of the events in the signal MC sample $H \rightarrow 2\gamma_d + X$ with $m_H = 125$ GeV. Events are classified as one of the three following channels:

- μDPJ–μDPJ,
- μDPJ–hDPJ,
- hDPJ–hDPJ.

In the μDPJ–hDPJ channel, either the μDPJ or the hDPJ may be the leading DPJ.

7 Multi-jet background estimation

A data-driven ABCD method is used to estimate the multi-jet background in each of the three channels. The ABCD method uses two nearly uncorrelated variables defined at the event level to create a two-dimensional plane that is split into four parts: region A, where most signal events are located, and three control regions (B, C, and D) that contain mostly background. The number of background events in A can be predicted from the population of the other three regions: $N_A = N_B \times N_D/N_C$, assuming negligible leakage of signal into regions B, C and D. For each channel, the ABCD calculation is performed in two separate regions: one background-dominated validation region (VR) to test the validity of the method, and one signal region (SR). The SRs are defined by the selection criteria described in Sects. 5 and 6. These define also the VRs except for the BDT cuts. The VRs BDT cuts for the leading and the subleading DPJs are chosen to have negligible signal contamination, which otherwise can bias the ABCD method validation. SR and VR definitions are summarised in Table 2.

The two event-level variables used to define the ABCD plane are the isolation of the DPJs relative to tracks in the inner detector and the opening angle between the two DPJs in the transverse plane ($|\Delta\phi|$). Displaced DPJs are expected to be highly isolated in the ID. The track isolation ($\sum p_T$) is defined as the scalar sum of the transverse momenta of the tracks reconstructed in the ID and matched to the PV of the event within a $\Delta R = 0.4$ cone around the DPJ direction. Matching to the PV helps reduce the dependence of $\sum p_T$ on the amount of pile-up. The PV is correctly selected in the $\sim 56\%$ of the events. However, the selection efficiency does not depend significantly on whether the PV is correctly identified. The larger of the two $\sum p_T$ values, $\max(\Sigma p_T)$, is used as the event-level variable. For signal, the opening angle $|\Delta\phi|$ is expected to be large, due to production of the DPJs in the two-body decay of a Higgs boson generated at rest in the transverse plane.

The ABCD method relies on there being only one source of background, or multiple sources that have identical distributions in the ABCD plane. Muons from BIB originate from beam-halo interactions with the collimators upstream of the ATLAS detector, resulting in muons travelling parallel to the beam-pipe. The analysis requirements select events with two separate energy deposits in the hadronic calorimeter produced by two BIB muons. The requirement $|\Delta\phi| > 0.1$ in the ABCD plane removes BIB events that would otherwise contaminate the method for the hDPJ–hDPJ channel, and has no effect on the signal efficiency. After the final selection, the contribution of BIB events to the signal region is negligible.

The ABCD plane is defined for all the three channels by $0 \leq \max(\Sigma p_T) \leq 20$ GeV and $0.1 \leq |\Delta\phi| \leq \pi$. The region A is defined by $\max(\Sigma p_T) < 4.5$ GeV and $|\Delta\phi| > 0.625$. Regions B, C, and D are defined by reversing one or both of the requirements: $\max(\Sigma p_T) > 4.5$ GeV and $|\Delta\phi| > 0.625$, $\max(\Sigma p_T) > 4.5$ GeV and $|\Delta\phi| < 0.625$, $\max(\Sigma p_T) < 4.5$ GeV and $|\Delta\phi| < 0.625$ respectively.

In order to estimate the residual cosmic-ray background component in the ABCD plane, the event selection is applied to the cosmic dataset, and the resulting event yield is multiplied by F_{CR}. The expected number of cosmic-ray events in the validation regions is: 4 ± 3 in region A and 2 ± 2 in region D for the μDPJ–μDPJ channel; 10 ± 5 in region D for the μDPJ–hDPJ channel. In the signal regions, the expected number of cosmic-ray events is: 8 ± 4 in region A and 2 ± 2 in region D for both the μDPJ–μDPJ and the μDPJ–hDPJ channel; 2 ± 2 in region A for the hDPJ–hDPJ channel. No

Table 3 Event count in each of the four regions of the ABCD plane in the validation regions and expected number of background events in region A. Only statistical uncertainties are shown. The expected contribution from cosmic rays is included in all regions and in the background estimation

DPJ pair type	B	C	D	Expected background in A	A
μDPJ–μDPJ	4	15	61	20 ± 10	17
μDPJ–hDPJ	455	87	318	1611 ± 227	1573
hDPJ–hDPJ	2556	536	14	67 ± 18	57

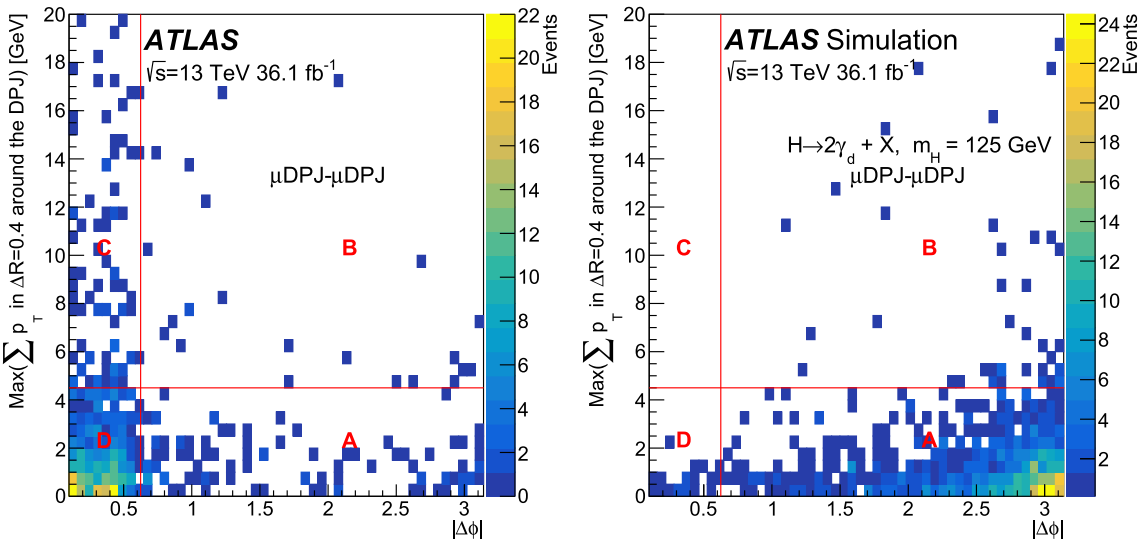

Fig. 3 Opening angle between the two DPJs, $|\Delta\phi|$, vs inner-detector isolation, $\max(\Sigma p_{\mathrm{T}})$, in the μDPJ–μDPJ channel for data (left) and MC signal $H \rightarrow 2\gamma_{\mathrm{d}} + X$ with $m_H = 125$ GeV (right), assuming a 10% Higgs boson decay branching fraction into γ_{d}. The red (solid) lines show the boundaries of the ABCD regions

events are observed in the remaining regions in the cosmic dataset. The estimated cosmic-ray event yields are subtracted from each of the ABCD regions before using the method to estimate the multi-jet background yield.

Other potential backgrounds to the signal include all the processes that lead to real prompt muons and muons plus jets in the final state, such as the SM production of W+jets, Z+jets, $t\bar{t}$, single-top-quark, WW, WZ, and ZZ events. MC samples are used to study these processes. They give no contribution after the trigger selection and the definition of muonic-DPJ and hadronic-DPJ and do not enter in the ABCD plane.

The signal contamination in the VRs is verified to be less than 5% for all channels. The linear correlation coefficient between the $\max(\Sigma p_{\mathrm{T}})$ and $|\Delta\phi|$ variables is verified to be less than 6% in the VR data, as well as in the SR using multi-jet MC events. The effect of this correlation on the final result is found to be negligible compared to the statistical accuracy. Table 3 shows the event counts in each of the four regions of the ABCD plane in the validation regions and the expected number of background events in the validation region A in data. Only statistical uncertainties are shown. The expected contribution from cosmic rays is included in all regions and in the background estimation. The observed number of events in the validation region A is in agreement with the number predicted by the ABCD method within the statistical uncertainties.

As additional validation of the ABCD method, control region D of the SR is divided into four subregions. The subregion with low $\max(\Sigma p_{\mathrm{T}})$ and high $|\Delta\phi|$ is treated as a mock signal region, with the other subregions serving as control regions. Applying the method, the expected and the observed numbers of events in the mock signal region are: 231 ± 58 and 184 for the μDPJ–μDPJ channel, 131 ± 41 and 145 for the μDPJ–hDPJ channel, 402 ± 77 and 479 for the hDPJ–hDPJ channel. These are in agreement within the statistical uncertainties.

Figure 3 shows the distribution of events in the ABCD plane of the μDPJ–μDPJ channel in the SR for the collision data and the MC signal $H \rightarrow 2\gamma_{\mathrm{d}} + X$ with $m_H = 125$ GeV, assuming a 10% Higgs boson decay branching fraction into γ_{d}. As a reference, the boundaries defining regions A, B, C and D are indicated in the figure by solid red lines.

In order to take into account the small signal contamination in regions B, C and D, a likelihood-based ABCD method

is used for the background estimation in the SR. It estimates the background in region A by performing a fit to the background and signal yields in the four regions. A likelihood function is formed from the product of four Poisson functions, one for each of the A, B, C, and D regions, describing signal and background expectations. The likelihood takes the form:

$$\mathcal{L}(n_{\mathrm{A}}, n_{\mathrm{B}}, n_{\mathrm{C}}, n_{\mathrm{D}}|s, b, \tau_{\mathrm{B}}, \tau_{\mathrm{C}}) = \prod_{i=\mathrm{A,B,C,D}} \frac{\mathrm{e}^{-N_i} N_i^{n_i}}{n_i!} \quad ,$$

where $n_{\mathrm{A}}, n_{\mathrm{B}}, n_{\mathrm{C}}$ and n_{D} are the four observables that denote the number of events observed in each region in data. The N_i are linear combinations of the signal and background expectation in each region, defined as follows:

$$\begin{aligned} N_{\mathrm{A}} &= s + b \\ N_{\mathrm{B}} &= s\,\varepsilon_{\mathrm{B}} + b\,\tau_{\mathrm{B}} \\ N_{\mathrm{C}} &= s\,\varepsilon_{\mathrm{C}} + b\,\tau_{\mathrm{C}} \\ N_{\mathrm{D}} &= s\,\varepsilon_{\mathrm{D}} + b\,\tau_{\mathrm{C}} \,/\, \tau_{\mathrm{B}} \end{aligned}$$

where s (b) is the signal (background) yield in region A, ε_i is the signal contamination derived from MC simulation, and τ_{B} and τ_{C} are the nuisance parameters that describe the ratio of the background expectation in the control region to the background expectation in the signal region. The s, b, τ_{B} and τ_{C} values are allowed to float in the fit to the four data regions.

8 Systematic uncertainties

The uncertainty in the ABCD-method background estimate is evaluated from the impact of a possible correlation between the ABCD variables in the SR. The correlation is evaluated using multi-jet MC events and validated in VR data. This effect is found to lead to a potential variation of less than 4% in the background estimate. The size of this uncertainty is therefore considered negligible when compared to the statistical one and it is not included in the fit.

The following effects are considered as possible sources of systematic uncertainty in the signal.

Luminosity
The uncertainty in the combined 2015–2016 integrated luminosity is 2.1% [95], obtained using the LUCID-2 detector [96] for the primary luminosity measurements.

Trigger
The systematic uncertainty in the narrow-scan trigger efficiency is evaluated using a tag-and-probe method applied to $J/\psi \to \mu\mu$ events in data and simulation. The difference between the trigger efficiency in data and that in simulation is evaluated as a function of the opening angle between the two muons. The difference in the region $\Delta R < 0.05$, corresponding to the ΔR expected for signal, is taken as the uncertainty and is 6%. The systematic uncertainty in the tri-muon MS-only trigger efficiency is 5.8%, taken from the analysis of 2012 data [11] since the algorithm has not undergone a major change since then. The systematic uncertainty in the CalRatio trigger efficiency is taken from Ref. [97] and is 2%.

BDT shape
The systematic uncertainty in the MC modelling of the input variables used for the BDT training is evaluated for both the μDPJ and the hDPJ. For the μDPJ, the data-to-MC ratio is computed for muon timing and z_0 BDT input variables using samples of $Z \to \mu\mu$ events. This comparison relies on the fact that, due to the high boost of low-mass dark photons and the high p_{T} of signal muons, the muon z_0 and timing distributions are similar to those of prompt muons from $Z \to \mu\mu$. Muons from Z boson decay are reconstructed using information only from the MS. The BDT is retrained using MC signal variables scaled to the data using these ratios, and the fit procedure is repeated. The resulting change in the final signal yield is taken as the systematic uncertainty, and its value is 3%. The same procedure is used for the hDPJ, where the ratios of data to simulated distributions are computed from data and MC samples of multi-jet events. The resulting uncertainty is 14%.

Muon reconstruction
The systematic uncertainty in the single-γ_{d} reconstruction efficiency is evaluated using a tag-and-probe method applied to $J/\psi \to \mu\mu$ events in 2015 data and simulation. $J/\psi \to \mu\mu$ decays are selected, and the efficiency is evaluated as a function of the opening angle ΔR between the two muons, for both the data and simulated J/ψ decays. For low ΔR values, the efficiency decreases due to the difficulty of reconstructing two tracks with small angular separation in the MS. The difference in $J/\phi \to \mu\mu$ reconstruction efficiency between simulation and data in the ΔR interval between 0 and 0.06 (where the DPJ samples are concentrated) amounts to 15%, and is taken as the uncertainty.

Jet energy scale and jet energy resolution
The jet energy scale and jet energy resolution introduce uncertainties in the signal yield of 1–8% and 1–5% respectively, depending on the signal process, where the processes with two dark photons are less affected. These uncertainties are calculated using the procedure detailed in Ref. [98]. Since the jets used in this analysis are required to have a low fraction of energy in the electromagnetic calorimeter, additional jet energy uncertainties are derived as a function of electromagnetic energy fraction as well as of pseudorapidity. These additional jet energy uncertainties are found to have an effect of up to 4% on the signal yield, and are taken in quadrature with the regular jet energy uncertainties.

Table 4 Observed numbers of events in the ABCD regions and expected number of background events in region A. In the estimate, the data in region A are not considered and the signal strength is fixed to zero. Both the statistical and systematic uncertainties in the background expectations are given. The expected contribution from cosmic rays is included in all regions

DPJ pair type	B	C	D	Expected A	A
μDPJ–μDPJ	24	92	463	128 ± 26 (stat.)	113
μDPJ–hDPJ	8	2	45	177 ± 86 (stat.)	179
hDPJ–hDPJ	13	2	15	97 ± 48 (stat.)	69

Table 5 Expected numbers of signal events in region A. A branching fraction value of $\mathcal{B}(H \to f_{\mathrm{d}_2}\,\bar{f}_{\mathrm{d}_2}) = 10\%$ is assumed for DPJ production in the decay of the $m_H = 125$ GeV Higgs boson. For DPJ production in the decay of a $m_H = 800$ GeV BSM scalar boson, a value of $\mathcal{B}(H \to f_{\mathrm{d}_2}\,\bar{f}_{\mathrm{d}_2}) = 100\%$ and a production cross section of $\sigma = 5$ pb are assumed. Only statistical uncertainties are reported

DPJ pair type	$m_H = 125$ GeV $H \to 2\gamma_{\mathrm{d}} + X$	$m_H = 125$ GeV $H \to 4\gamma_{\mathrm{d}} + X$	$m_H = 800$ GeV $H \to 2\gamma_{\mathrm{d}} + X$	$m_H = 800$ GeV $H \to 4\gamma_{\mathrm{d}} + X$
μDPJ–μDPJ	639 ± 25	519 ± 23	610 ± 87	660 ± 91
μDPJ–hDPJ	74 ± 9	22 ± 5	1544 ± 139	996 ± 111
hDPJ–hDPJ	8 ± 3	0	560 ± 84	336 ± 65

Effect of pile-up on ΣpT

The presence of multiple collisions per bunch crossing affects the efficiency of the ID track isolation criterion quantified in terms of Σp_{T}. The systematic uncertainty is evaluated by comparing Σp_{T} for muons from a sample of reconstructed $Z \to \mu\mu$ events in data with that in simulation, as a function of the number of interaction vertices in the event. The systematic uncertainty is evaluated as the maximum difference at the value of the selection requirement on $\max(\Sigma p_{\mathrm{T}})$. It is found to be 5.1%.

9 Results and interpretation

The observed numbers of events in the ABCD regions and the expected number of background events in the signal region A are summarised in Table 4. The expected number of background events in region A is estimated using the likelihood-based ABCD method, assuming no signal and not including the observed data in region A. The background estimate includes both the multi-jet and cosmic-ray background, where the former is obtained as described in Sect. 7, and the latter is estimated from the cosmic dataset. Both sources are included in the expected background given in Table 4. The observed number of events in region A is in agreement with the predicted number of background events.

Table 5 shows the expected number of signal events in region A for the FRVZ model parameters of Table 1 and the following assumptions: a value of $\mathcal{B}(H \to f_{\mathrm{d}_2}\,\bar{f}_{\mathrm{d}_2}) = 10\%$ for a Higgs boson with $m_H = 125$ GeV, which is not excluded by the current measurements [5]; a value of $\mathcal{B}(H \to f_{\mathrm{d}_2}\,\bar{f}_{\mathrm{d}_2}) = 100\%$ and a production cross section of $\sigma = 5$ pb for a BSM scalar boson with $m_H = 800$ GeV.

Upper limits on the production cross section times branching fraction ($\sigma \times \mathcal{B}$) as a function of the γ_{d} proper decay length are derived for the FRVZ $H \to 2\gamma_{\mathrm{d}} + X$ and $H \to 4\gamma_{\mathrm{d}} + X$ processes using the $\mathrm{CL_s}$ method [99]. Since each signal sample was generated for a particular proper decay length, it is necessary to extrapolate the signal efficiency to other decay lengths to obtain limits as a function of $c\tau$. This is achieved by applying to the i-th dark photon in the event a weight

$$w_i(t_i) = \frac{\tau_{\mathrm{ref}}}{\mathrm{e}^{-t_i/\tau_{\mathrm{ref}}}} \cdot \frac{\mathrm{e}^{-t_i/\tau_{\mathrm{new}}}}{\tau_{\mathrm{new}}},$$

where τ_{ref} is the lifetime with which the event sample was simulated, τ_{new} is the lifetime for which it is weighted, and t_i is the proper decay time of the i-th dark photon. Each event is weighted by the product of the individual dark-photon weights. The weighted sample is used to evaluate the signal efficiency for τ_{new}. Figure 4 shows the extrapolated signal efficiency for the $H \to 2\gamma_{\mathrm{d}} + X$ and $H \to 4\gamma_{\mathrm{d}} + X$ processes as a function of $c\tau$ of the dark photon in the μDPJ–μDPJ, μDPJ–hDPJ and hDPJ–hDPJ channels. The tri-muon MS-only trigger has a lower efficiency for the $H \to 2\gamma_{\mathrm{d}} + X$ process with a $m_H = 125$ GeV Higgs boson than for the other processes, resulting in a lower signal efficiency in the μDPJ–μDPJ channel. The p_{T} requirements of the CalRatio trigger are not optimal for selecting jets produced by γ_{d} decays in the processes with a $m_H = 125$ GeV Higgs boson, resulting in a signal efficiency below 1% in the hDPJ–hDPJ channel. The muon narrow-scan trigger helps to recover some efficiency in the μDPJ–hDPJ channel for these processes.

The observed 95% CL cross-section upper limits in the μDPJ–μDPJ channel for the $H \to 2\gamma_{\mathrm{d}} + X$ and $H \to 4\gamma_{\mathrm{d}} + X$ processes are presented in Fig. 5 for

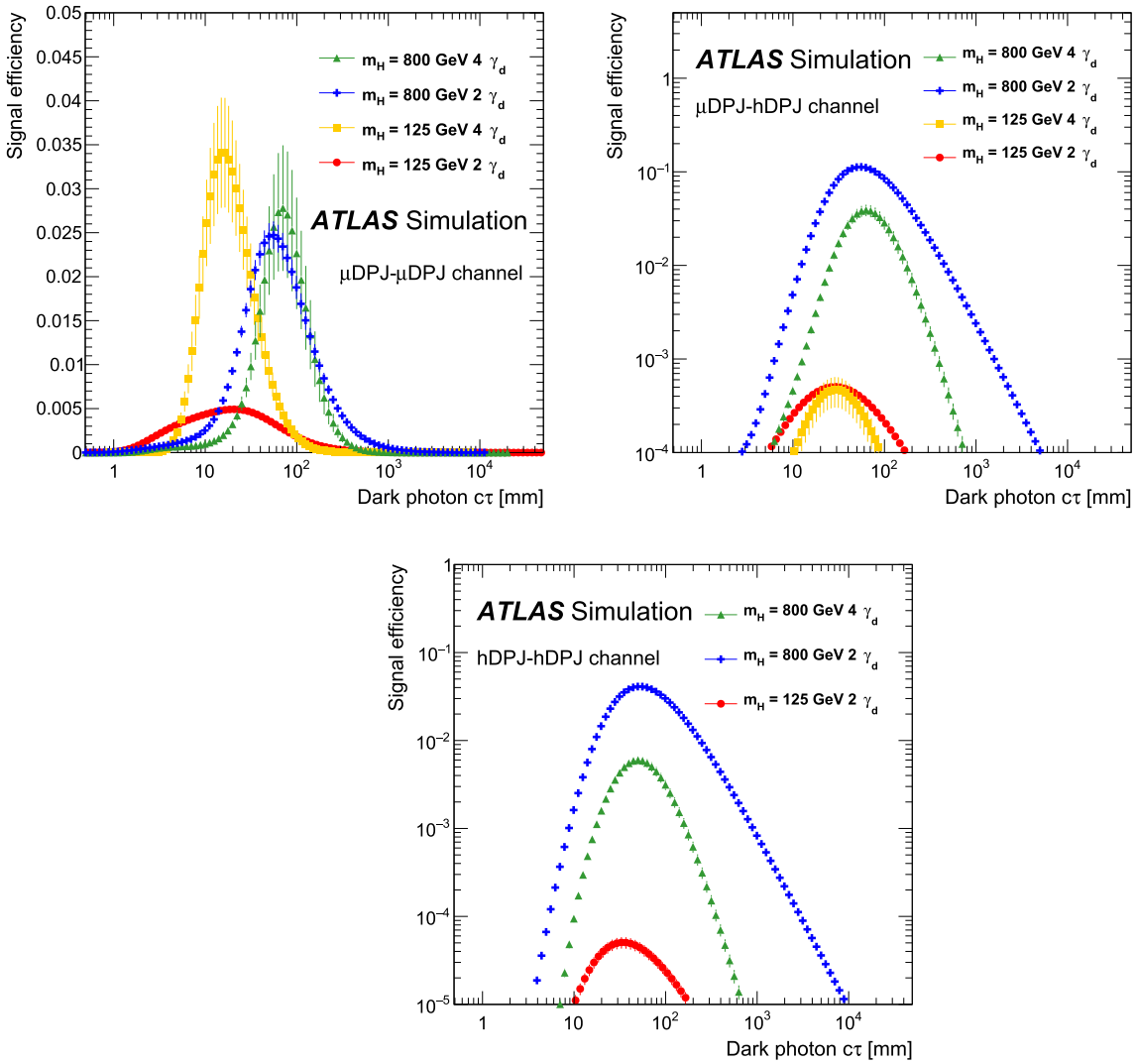

Fig. 4 Extrapolated signal efficiencies as a function of proper decay length of the γ_{d} for the $H \to 2\gamma_{\mathrm{d}} + X$ and $H \to 4\gamma_{\mathrm{d}} + X$ processes and for the three different channels: μDPJ–μDPJ (left), μDPJ–hDPJ (right) and hDPJ–hDPJ (bottom). The signal efficiency in the hDPJ–hDPJ channel for $m_H = 125$ GeV $H \to 4\gamma_{\mathrm{d}} + X$ process is small compared with the other channels and is not shown. The vertical bars represent the statistical uncertainties

$m_H = 125$ GeV. The 95% CL exclusion limits in the μDPJ–μDPJ and hDPJ–hDPJ channels for the process $H \to 2\gamma_{\mathrm{d}} + X$ are presented in Fig. 6 for $m_H = 800$ GeV. The figures also show the expected limits obtained from the likelihood-based ABCD method, using the background estimate derived from the background-only fit using data in the four regions. Excluded $c\tau$ ranges are summarised in Table 6, assuming $\mathcal{B}(H \to f_{\mathrm{d}_2}\, \bar{f}_{\mathrm{d}_2}) = 10\%$ for the Higgs boson with $m_H = 125$ GeV and $\mathcal{B}(H \to f_{\mathrm{d}_2}\, \bar{f}_{\mathrm{d}_2}) = 100\%$ for the BSM Higgs boson, with subsequent decay of the f_{d_2} and $\bar{f}_{\mathrm{d}_2}$ giving rise to the production of two or four dark photons.

The results for the μDPJ–μDPJ channel is also interpreted in terms of the kinetic mixing parameter ϵ and γ_{d} mass, shown in Fig. 7 as exclusion contours. These limits assume four possible values of the Higgs boson decay branching fractions into γ_{d}, ranging from 1 to 20%, and the NNLO gluon–gluon fusion Higgs boson production cross section. The γ_{d} detection efficiency for a γ_{d} mass of 0.4 GeV is used for the mass interval 0.25–2 GeV, as the detection efficiency is constant throughout this interval [11]. The decay branching fraction variations as a function of the γ_{d} mass are estimated and included in the 90% CL exclusion region evaluations [56]. The low sensitivity in the hDPJ–hDPJ channel prevents the exclusion of the mass regions where the γ_{d} decays into hadronic resonances: γ_{d} mass regions around 0.8 and 1.0 GeV, where the γ_{d} decays into the ρ, ω, and ϕ resonances. Figure 7 also shows previous exclusions for a Higgs boson decay branching fractions into γ_{d} of 10% from a search

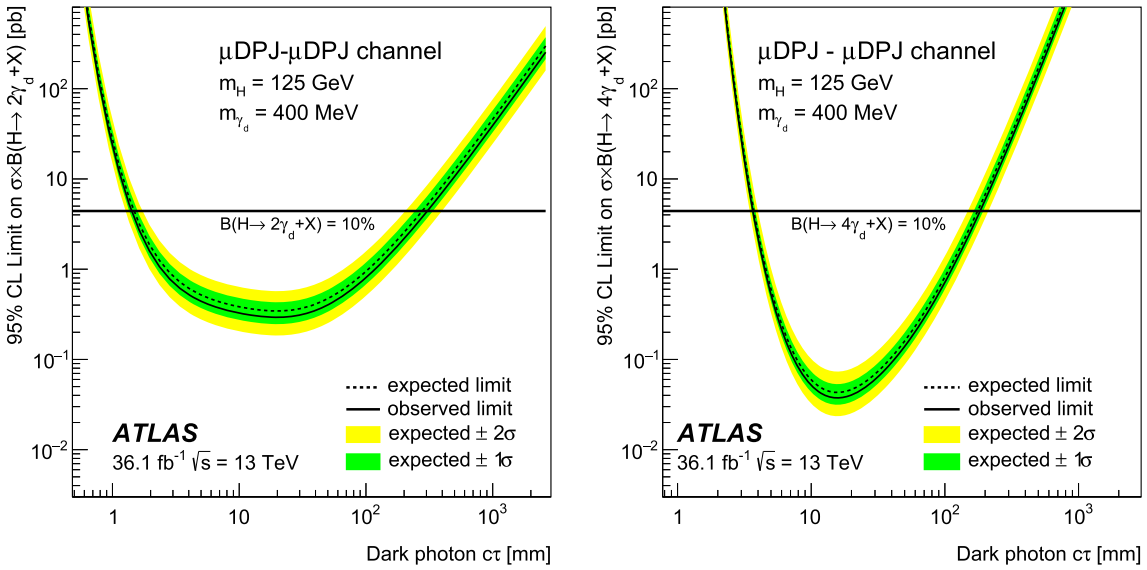

Fig. 5 Upper limits at 95% CL on the cross section times branching fraction for the processes $H \rightarrow 2\gamma_{\mathrm{d}} + X$ (left) and $H \rightarrow 4\gamma_{\mathrm{d}} + X$ (right) in the μDPJ–μDPJ final states for $m_H = 125$ GeV. The horizontal lines correspond to the cross section times branching fraction for a value of the branching fraction of the Higgs boson decay into dark fermions of 10%

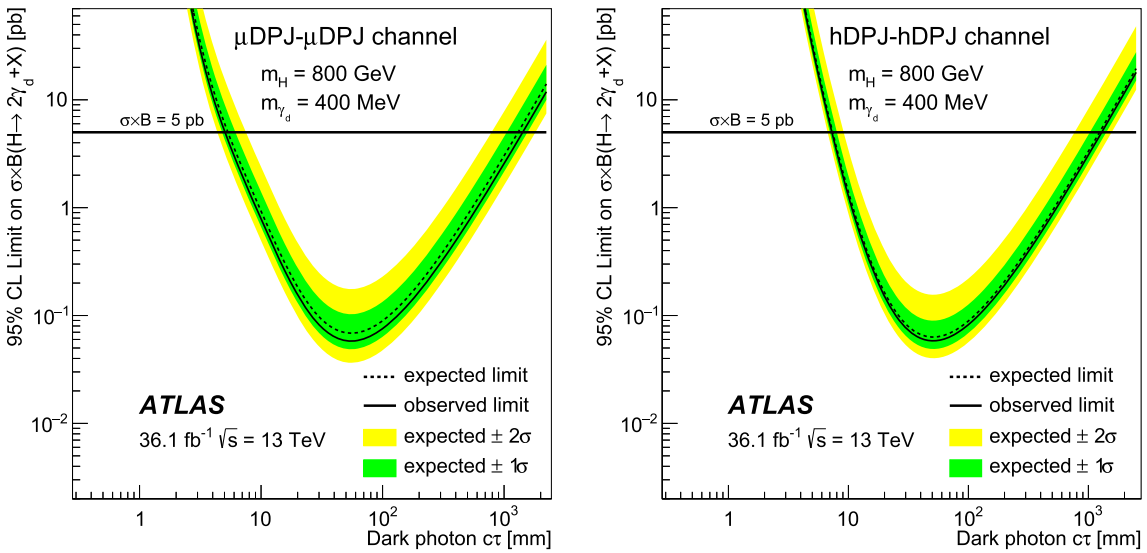

Fig. 6 Upper limits at 95% CL on the cross section times branching fraction for the process $H \rightarrow 2\gamma_{\mathrm{d}} + X$, where H is an 800 GeV BSM Higgs boson, in the μDPJ–μDPJ (left) and hDPJ–hDPJ (right) final states. The horizontal lines correspond to a cross section times branching fraction of 5 pb

Table 6 Ranges of γ_{d} cτ excluded at 95% CL for $H \rightarrow 2\gamma_{\mathrm{d}} + X$ and $H \rightarrow 4\gamma_{\mathrm{d}} + X$. A branching fraction value of $\mathcal{B}(H \rightarrow f_{\mathrm{d}_2}\,\bar{f}_{\mathrm{d}_2}) = 10\%$ is assumed for DPJ production in the decay of a $m_H = 125$ GeV Higgs boson. For DPJ production in the decay of a $m_H = 800$ GeV BSM scalar boson, a value of $\mathcal{B}(H \rightarrow f_{\mathrm{d}_2}\,\bar{f}_{\mathrm{d}_2}) = 100\%$ and a production cross section of $\sigma = 5$ pb are assumed

Model	Excluded cτ [mm] $m_H = 125$ GeV $H \rightarrow 2\gamma_{\mathrm{d}} + X$	Excluded cτ [mm] $m_H = 125$ GeV $H \rightarrow 4\gamma_{\mathrm{d}} + X$	Excluded cτ [mm] $m_H = 800$ GeV $H \rightarrow 2\gamma_{\mathrm{d}} + X$	Excluded cτ [mm] $m_H = 800$ GeV $H \rightarrow 4\gamma_{\mathrm{d}} + X$
μDPJ–μDPJ	$1.5 \leq c\tau \leq 307$	$3.7 \leq c\tau \leq 178$	$5.0 \leq c\tau \leq 1420$	$10.5 \leq c\tau \leq 312$
μDPJ–hDPJ	–	–	$7.2 \leq c\tau \leq 1234$	$14.5 \leq c\tau \leq 334$
hDPJ–hDPJ	–	–	$7.3 \leq c\tau \leq 1298$	$13.6 \leq c\tau \leq 231$

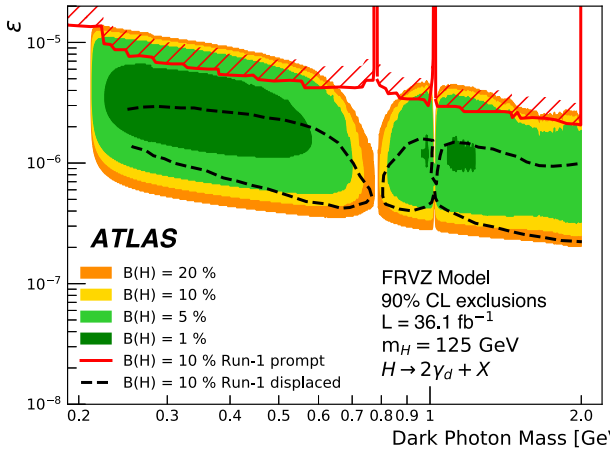

Fig. 7 The 90% CL exclusion regions for the decay $H \to 2\gamma_{\mathrm{d}} + X$ of the Higgs boson as a function of the γ_{d} mass and of the kinetic mixing parameter ϵ. These limits are obtained assuming the FRVZ model with decay branching fractions of the Higgs boson into γ_{d} between 1 and 20%, and the NNLO Higgs boson production cross sections via gluon–gluon fusion. The figure also shows excluded regions with decay branching fraction of the Higgs boson into γ_{d} of 10% from the run-1 ATLAS displaced [11] (black line) and prompt [14] (red line) dark-photon jets searches

for displaced dark-photon jets [11] and prompt dark-photon jets [14] at ATLAS. The search of Ref. [11], which explored the same region probed by this analysis, is slightly more sensitive in the region of high γ_{d} mass and low ϵ. This is due to inclusion of dark-photon jets with both muon and hadron constituents, which are not used in the current analysis. The search of Ref. [14] excluded high ϵ values (shorter lifetimes), a region complementary to this analysis.

10 Conclusions

The ATLAS detector at the LHC is used to search for the production of displaced dark-photon jets in a sample of pp collisions at $\sqrt{s} = 13$ TeV corresponding to an integrated luminosity of 36.1 fb^{-1}. No significant excess of events compared with the background expectation is observed, and 95% confidence-level upper limits are set on the production cross section times branching fraction of scalar bosons that decay into dark photons according to the FRVZ model. The upper limits are computed as a function of the proper decay length $c\tau$ of the dark photon γ_{d}. In addition to the increase in integrated luminosity and centre-of-mass energy, improvements in background suppression and the exploitation of hadronic γ_{d} decays result in increased sensitivity compared with the ATLAS search using 8 TeV pp data. In the pure muonic channel, assuming a branching ratio $\mathcal{B}(H \to 2(4)\gamma_{\mathrm{d}} + X) = 10\%$ for $m_H = 125$ GeV, decays of dark photons are excluded at 95% CL for $c\tau \in [1.5, 307]$ mm and $c\tau \in [3.7, 178]$ mm for production of two and four dark photons, respectively. For $m_H = 800$ GeV, assuming $\sigma \times \mathcal{B}(H \to 2(4)\gamma_{\mathrm{d}} + X) = 5$ pb, the excluded regions are $c\tau \in [5, 1420]$ mm and $c\tau \in [10.5, 312]$ mm. In the pure hadronic channel, the $m_H = 800$ GeV excluded regions become $c\tau \in [7.3, 1298]$ mm and $c\tau \in [13.6, 231]$ mm.

The results for $H \to 2\gamma_{\mathrm{d}} + X$, when H is the Higgs boson, are also interpreted as 90% confidence-level limits on the kinetic mixing parameter as a function of the dark-photon mass. These results improve upon the constraints set in previous LHC searches.

Acknowledgements We thank CERN for the very successful operation of the LHC, as well as the support staff from our institutions without whom ATLAS could not be operated efficiently.
We acknowledge the support of ANPCyT, Argentina; YerPhI, Armenia; ARC, Australia; BMWFW and FWF, Austria; ANAS, Azerbaijan; SSTC, Belarus; CNPq and FAPESP, Brazil; NSERC, NRC and CFI, Canada; CERN; CONICYT, Chile; CAS, MOST and NSFC, China; COLCIENCIAS, Colombia; MSMT CR, MPO CR and VSC CR, Czech Republic; DNRF and DNSRC, Denmark; IN2P3-CNRS, CEA-DRF/IRFU, France; SRNSFG, Georgia; BMBF, HGF, and MPG, Germany; GSRT, Greece; RGC, Hong Kong SAR, China; ISF and Benoziyo Center, Israel; INFN, Italy; MEXT and JSPS, Japan; CNRST, Morocco; NWO, Netherlands; RCN, Norway; MNiSW and NCN, Poland; FCT, Portugal; MNE/IFA, Romania; MES of Russia and NRC KI, Russian Federation; JINR; MESTD, Serbia; MSSR, Slovakia; ARRS and MIZŠ, Slovenia; DST/NRF, South Africa; MINECO, Spain; SRC and Wallenberg Foundation, Sweden; SERI, SNSF and Cantons of Bern and Geneva, Switzerland; MOST, Taiwan; TAEK, Turkey; STFC, United Kingdom; DOE and NSF, USA. In addition, individual groups and members have received support from BCKDF, CANARIE, CRC and Compute Canada, Canada; COST, ERC, ERDF, Horizon 2020, and Marie Skłodowska-Curie Actions, European Union; Investissements d' Avenir Labex and Idex, ANR, France; DFG and AvH Foundation, Germany; Herakleitos, Thales and Aristeia programmes co-financed by EU-ESF and the Greek NSRF, Greece; BSF-NSF and GIF, Israel; CERCA Programme Generalitat de Catalunya, Spain; The Royal Society and Leverhulme Trust, United Kingdom. The crucial computing support from all WLCG partners is acknowledged gratefully, in particular from CERN, the ATLAS Tier-1 facilities at TRIUMF (Canada), NDGF (Denmark, Norway, Sweden), CC-IN2P3 (France), KIT/GridKA (Germany), INFN-CNAF (Italy), NL-T1 (Netherlands), PIC (Spain), ASGC (Taiwan), RAL (UK) and BNL (USA), the Tier-2 facilities worldwide and large non-WLCG resource providers. Major contributors of computing resources are listed in Ref. [100].

Data Availability Statement This manuscript has no associated data or the data will not be deposited. [Authors' comment: All ATLAS scientific output is published in journals, and preliminary results are made available in Conference Notes. All are openly available, without restriction on use by external parties beyond copyright law and the standard conditions agreed by CERN. Data associated with journal publications are also made available: tables and data from plots (e.g. cross section values, likelihood profiles, selection efficiencies, cross section limits, ...) are stored in appropriate repositories such as HEPDATA (http://hepdata.cedar.ac.uk/). ATLAS also strives to make additional material related to the paper available that allows a reinterpretation of the data in the context of new theoretical models. For example, an extended encapsulation of the analysis is often provided for measurements in the framework of RIVET (http://rivet.hepforge.org/..)]

Funded by SCOAP[3].

References

1. N. Arkani-Hamed, N. Weiner, LHC signals for a superunified theory of dark matter. JHEP **12**, 104 (2008). arXiv:0810.0714 [hep-ph]
2. M. Baumgart, C. Cheung, J.T. Ruderman, L.-T. Wang, I. Yavin, Non-abelian dark sectors and their collider signatures. JHEP **04**, 014 (2009). arXiv:0901.0283 [hep-ph]
3. A. Falkowski, R. Vega-Morales, Exotic Higgs decays in the golden channel. JHEP **12**, 037 (2014). arXiv:1405.1095 [hep-ph]
4. D. Curtin, R. Essig, S. Gori, J. Shelton, Illuminating dark photons with high-energy colliders. JHEP **02**, 157 (2015). arXiv:1412.0018 [hep-ph]
5. ATLAS Collaboration, Combination of searches for invisible Higgs boson decays with the ATLAS experiment, Phys. Rev. Lett. **122**, 231801 (2019). arXiv:1904.05105 [hep-ex]
6. CMS Collaboration, Search for invisible decays of a Higgs boson produced through vector boson fusion in proton-proton collisions at $\sqrt{s} = 13$ TeV. Phys. Lett. B **793**, 520 (2019). arXiv:1809.05937 [hep-ex]
7. C. Cheung, J.T. Ruderman, L.-T. Wang, I. Yavin, Lepton jets in (supersymmetric) electroweak processes. JHEP **04**, 116 (2010). arXiv:0909.0290 [hep-ph]
8. A. Falkowski, J.T. Ruderman, T. Volansky, J. Zupan, Hidden Higgs decaying to lepton jets. JHEP **05**, 077 (2010). arXiv:1002.2952 [hep-ph]
9. A. Falkowski, J.T. Ruderman, T. Volansky, J. Zupan, Discovering Higgs boson decays to lepton jets at hadron colliders. Phys. Rev. Lett. **105**, 241801 (2010). arXiv:1007.3496 [hep-ph]
10. ATLAS Collaboration, Search for displaced muonic lepton jets from light Higgs boson decay in proton–proton collisions at $\sqrt{s} =$ 7 TeV with the ATLAS detector. Phys. Lett. B **721**, 32 (2013). arXiv:1210.0435 [hep-ex]
11. ATLAS Collaboration, Search for long-lived neutral particles decaying into lepton jets in proton–proton collisions at $\sqrt{s} = 8$ TeV with the ATLAS detector. JHEP **11**, 088 (2014). arXiv:1409.0746 [hep-ex]
12. ATLAS Collaboration, Search for WH production with a light Higgs boson decaying to prompt electron-jets in proton–proton collisions at $\sqrt{s} = 7$ TeV with the ATLAS detector. New J. Phys. **15**, 043009 (2013). arXiv:1302.4403 [hep-ex]
13. ATLAS Collaboration, A search for prompt lepton-jets in pp collisions at $\sqrt{s} = 7$ TeV with the ATLAS detector. Phys. Lett. B **719**, 299 (2013). arXiv:1212.5409 [hep-ex]
14. ATLAS Collaboration, A search for prompt lepton-jets in pp collisions at $\sqrt{s} = 8$ TeV with the ATLAS detector. JHEP **02**, 062 (2016). arXiv:1511.05542 [hep-ex]
15. ATLAS Collaboration, Search for long-lived particles in final states with displaced dimuon vertices in pp collisions at $\sqrt{s} =$ 13 TeV with the ATLAS detector. Phys. Rev. D **99**, 012001 (2019). arXiv:1808.03057 [hep-ex]
16. CDF Collaboration, Search for anomalous production of multiple leptons in association with W and Z bosons at CDF. Phys. Rev. D **85**, 092001 (2012). arXiv:1202.1260 [hep-ex]
17. D0 Collaboration, Search for dark photons from supersymmetric hidden valleys. Phys. Rev. Lett. **103**, 081802 (2009). arXiv:0905.1478 [hep-ex]
18. D0 Collaboration, Search for events with leptonic jets and missing transverse energy in $p\bar{p}$ collisions at $\sqrt{s} = 1.96$ TeV. Phys. Rev. Lett. **105**, 211802 (2010). arXiv:1008.3356 [hep-ex]
19. CMS Collaboration, Search for light resonances decaying into pairs of muons as a signal of new physics. JHEP **07**, 098 (2011). arXiv:1106.2375 [hep-ex]
20. CMS Collaboration, Search for a non-standard-model Higgs boson decaying to a pair of new light bosons in four-muon final states. Phys. Lett. B **726**, 564 (2013). arXiv:1210.7619 [hep-ex]
21. CMS Collaboration, A search for pair production of new light bosons decaying into muons. Phys. Lett. B **752**, 146 (2016). arXiv:1506.00424 [hep-ex]
22. CMS Collaboration, Search for dark photons in decays of Higgs bosons produced in association with Z bosons in proton-proton collisions at $\sqrt{s} = 13$ TeV (2019). arXiv:1908.02699 [hep-ex]
23. LHCb Collaboration, Search for hidden-sector bosons in $B^0 \to K^{*0}\mu^+\mu^-$ decays. Phys. Rev. Lett. **115**, 161802 (2015). arXiv:1508.04094 [hep-ex]
24. LHCb Collaboration, Search for dark photons produced in 13 TeV pp collisions. Phys. Rev. Lett. **120**, 061801 (2018). arXiv:1710.02867 [hep-ex]
25. J. Blümlein, J. Brunner, New exclusion limits for dark gauge forces from beam-dump data. Phys. Lett. B **701**, 155 (2011). arXiv:1104.2747 [hep-ex]
26. J.D. Bjorken, R. Essig, P. Schuster, N. Toro, New fixed-target experiments to search for dark gauge forces. Phys. Rev. D **80**, 075018 (2009). arXiv:0906.0580 [hep-ph]
27. A. Bross et al., Search for short-lived particles produced in an electron beam dump. Phys. Rev. Lett. **67**, 2942 (1991)
28. A1 Collaboration, Search for Light gauge bosons of the dark sector at the mainz microtron. Phys. Rev. Lett. **106**, 251802 (2011). arXiv:1101.4091 [nucl-ex]
29. WASA-at-COSY Collaboration, Search for a dark photon in the $\pi^0 \to e^+e^-\gamma$ decay. Phys. Lett. B **726**, 187 (2013). arXiv:1304.0671 [hep-ex]
30. APEX Collaboration, Search for a new gauge boson in electron-nucleus fixed-target scattering by the APEX experiment. Phys. Rev. Lett. **107**, 191804 (2011). arXiv:1108.2750 [hep-ex]
31. M. Reece, L.-T. Wang, Searching for the light dark gauge boson in GeV-scale experiments. JHEP **07**, 051 (2009). arXiv:0904.1743 [hep-ph]
32. J. Blümlein, J. Brunner, New exclusion limits on dark gauge forces from proton Bremsstrahlung in beam-dump data. Phys. Lett. B **731**, 320 (2014). arXiv:1311.3870 [hep-ph]
33. S.N. Gninenko, Constraints on sub-GeV hidden sector gauge bosons from a search for heavy neutrino decays. Phys. Lett. B **713**, 244 (2012). arXiv:1204.3583 [hep-ph]
34. R. Essig, R. Harnik, J. Kaplan, N. Toro, Discovering new light states at neutrino experiments. Phys. Rev. D **82**, 113008 (2010). arXiv:1008.0636 [hep-ph]
35. HADES Collaboration, Searching a dark photon with HADES. Phys. Lett. B **731**, 265 (2014). arXiv:1311.0216 [hep-ex]
36. KLOE-2 Collaboration, Search for a vector gauge boson in ϕ meson decays with the KLOE detector. Phys. Lett. B **706**, 251 (2012). arXiv:1110.0411 [hep-ex]
37. KLOE-2 Collaboration, Limit on the production of a light vector gauge boson in ϕ meson decays with the KLOE detector. Phys. Lett. B **720**, 111 (2013). arXiv:1210.3927 [hep-ex]

38. BABAR Collaboration, Search for dimuon decays of a light scalar boson in radiative transitions $\Upsilon \to \gamma A^0$. Phys. Rev. Lett. **103**, 081803 (2009). arXiv:0905.4539 [hep-ex]
39. BABAR Collaboration, Search for a dark photon in e^+e^- collisions at BaBar. Phys. Rev. Lett. **113**, 201801 (2014). arXiv:1406.2980 [hep-ex]
40. BABAR Collaboration, Search for long-lived particles in e^+e^- collisions. Phys. Rev. Lett. **114**, 171801 (2015). arXiv:1502.02580 [hep-ex]
41. Belle Collaboration, Search for the dark photon and the dark Higgs boson at Belle. Phys. Rev. Lett. **114**, 211801 (2015). arXiv:1502.00084 [hep-ex]
42. Belle Collaboration, Search for a dark vector gauge boson decaying to $\pi^+\pi^-$ using $\eta \to \pi^+\pi^-\gamma$ decays. Phys. Rev. D **94**, 092006 (2016). arXiv:1609.05599 [hep-ex]
43. BESSIII Collaboration, Measurement of $\mathcal{B}(J/\psi \to \eta' e^+e^-)$ and search for a dark photon. Phys. Rev. D **99**, 012013 (2019). arXiv:1809.00635 [hep-ex]
44. BESSIII Collaboration, Dark photon search in the mass range between 1.5 and 3.4 GeV/c^2. Phys. Lett. B **774**, 252 (2017). arXiv:1705.04265 [hep-ex]
45. M. Pospelov, Secluded U(1) below the weak scale. Phys. Rev. D **80**, 095002 (2009). arXiv:0811.1030 [hep-ph]
46. H. Davoudiasl, H.-S. Lee, W.J. Marciano, Dark side of Higgs diphoton decays and muon $g-2$. Phys. Rev. D **86**, 095009 (2012). arXiv:1208.2973 [hep-ph]
47. M. Endo, K. Hamaguchi, G. Mishima, Constraints on hidden photon models from electron $g-2$ and hydrogen spectroscopy. Phys. Rev. D **86**, 095029 (2012). arXiv:1209.2558 [hep-ph]
48. J.B. Dent, F. Ferrer, L.M. Krauss, Constraints on light hidden sector gauge bosons from supernova cooling (2012). arXiv:1201.2683 [astro-ph.CO]
49. H.K. Dreiner, J.-F. Fortin, C. Hanhart, L. Ubaldi, Supernova constraints on MeV dark sectors from e^+e^- annihilations. Phys. Rev. D **89**, 105015 (2014). arXiv:1310.3826 [hep-ph]
50. ATLAS Collaboration, The ATLAS Experiment at the CERN Large Hadron Collider, JINST 3, S08003 (2008)
51. ATLAS Collaboration, ATLAS Insertable B-Layer Technical Design Report, ATLAS-TDR-19, 2010, URL: https://cds.cern.ch/record/1291633, Addendum: ATLAS-TDR-19-ADD-1, 2012. https://cds.cern.ch/record/1451888
52. B. Abbott et al., Production and integration of the ATLAS Insertable B-Layer. JINST **13**, T05008 (2018). arXiv:1803.00844 [physics.ins-det]
53. ATLAS Collaboration, Performance of the ATLAS trigger system in 2015. Eur. Phys. J. C **77**, 317 (2017). arXiv:1611.09661 [hep-ex]
54. M.J. Strassler, K.M. Zurek, Echoes of a hidden valley at hadron colliders. Phys. Lett. B **651**, 374 (2007). arXiv:hep-ph/0604261
55. P. Meade, M. Papucci, T. Volansky, Dark matter sees the light. JHEP **12**, 052 (2009). arXiv:0901.2925 [hep-ph]
56. B. Batell, M. Pospelov, A. Ritz, Probing a secluded U(1) at B factories. Phys. Rev. D **79**, 115008 (2009). arXiv:0903.0363 [hep-ph]
57. C. Cheung, J.T. Ruderman, L.-T. Wang, I. Yavin, Kinetic mixing as the origin of a light dark-gauge-group scale. Phys. Rev. D **80**, 035008 (2009). arXiv:0902.3246 [hep-ph]
58. ATLAS Collaboration, Characterisation and mitigation of beam-induced backgrounds observed in the ATLAS detector during the 2011 proton–proton run, JINST 8, P07004 (2013). arXiv:1303.0223 [hep-ex]
59. S. Dittmaier et al., Handbook of LHC Higgs Cross Sections: 1. Inclusive Observables, CERN- 2011-002. arXiv:1101.0593 [hep-ph], https://cds.cern.ch/record/1318996
60. R.V. Harlander, W.B. Kilgore, Next-to-next-to-leading order Higgs production at hadron colliders. Phys. Rev. Lett. **88**, 201801 (2002). arXiv:hep-ph/0201206 [hep-ph]
61. C. Anastasiou, K. Melnikov, Higgs boson production at hadron colliders in NNLO QCD. Nucl. Phys. B **646**, 220 (2002). arXiv:hep-ph/0207004 [hep-ph]
62. V. Ravindran, J. Smith, W.L. van Neerven, NNLO corrections to the total cross-section for Higgs boson production in hadron hadron collisions. Nucl. Phys. B **665**, 325 (2003). arXiv:hep-ph/0302135 [hep-ph]
63. J. Alwall et al., The automated computation of tree-level and next-to-leading order differential cross sections, and their matching to parton shower simulations. JHEP **07**, 079 (2014). arXiv:1405.0301 [hep-ph]
64. T. Sjöstrand et al., An introduction to PYTHIA 8.2. Comput. Phys. Commun. **191**, 159 (2015). arXiv:1410.3012 [hep-ph]
65. ATLAS Collaboration, ATLAS Pythia 8 tunes to 7 TeV data, ATL-PHYS-PUB-2014-021, (2014). https://cds.cern.ch/record/1966419
66. R.D. Ball et al., Parton distributions with LHC data. Nucl. Phys. B **867**, 244 (2013). arXiv:1207.1303 [hep-ph]
67. T. Gleisberg et al., Event generation with SHERPA 1.1. JHEP **02**, 007 (2009). arXiv:0811.4622 [hep-ph]
68. R.D. Ball et al., Parton distributions for the LHC run II. JHEP **04**, 040 (2015). arXiv:1410.8849 [hep-ph]
69. P. Nason, A new method for combining NLO QCD with shower Monte Carlo algorithms. JHEP **11**, 040 (2004). arXiv:hep-ph/0409146
70. S. Frixione, P. Nason, C. Oleari, Matching NLO QCD computations with Parton Shower simulations: the POWHEG method. JHEP **11**, 070 (2007). arXiv:0709.2092 [hep-ph]
71. S. Alioli, P. Nason, C. Oleari, E. Re, NLO single-top production matched with shower in POWHEG: s- and t-channel contributions. JHEP **09**, 111 (2009), [Erratum: JHEP02, 011 (2010)]. arXiv:0907.4076 [hep-ph]
72. S. Frixione, G. Ridolfi, P. Nason, A positive-weight next-to-leading-order Monte Carlo for heavy flavour hadroproduction. JHEP **09**, 126 (2007). arXiv:0707.3088 [hep-ph]
73. T. Sjöstrand, S. Mrenna, P.Z. Skands, PYTHIA 6.4 physics and manual. JHEP **05**, 026 (2006). arXiv:hep-ph/0603175 [hep-ph]
74. P.Z. Skands, Tuning Monte Carlo generators: the Perugia tunes. Phys. Rev. D **82**, 074018 (2010). arXiv:1005.3457 [hep-ph]
75. H.-L. Lai et al., New parton distributions for collider physics. Phys. Rev. D **82**, 074024 (2010). arXiv:1007.2241 [hep-ph]
76. J. Pumplin et al., New generation of parton distributions with uncertainties from global QCD analysis. JHEP **07**, 012 (2002). arXiv:hep-ph/0201195
77. P. Golonka, Z. Was, PHOTOS Monte Carlo: a precision tool for QED corrections in Z and W decays. Eur. Phys. J. C **45**, 97 (2006). arXiv:hep-ph/0506026 [hep-ph]
78. ATLAS Collaboration, Muon reconstruction performance of the ATLAS detector in proton–proton collision data at $\sqrt{s} = 13$ TeV. Eur. Phys. J. C **76**, 292 (2016). arXiv:1603.05598 [hep-ex]
79. ATLAS Collaboration, The ATLAS simulation infrastructure. Eur. Phys. J. C **70**, 823 (2010). arXiv:1005.4568 [physics.ins-det]
80. S. Agostinelli et al., GEANT4: a simulation toolkit. Nucl. Instrum. Methods A **506**, 250 (2003)
81. ATLAS Collaboration, Summary of ATLAS Pythia 8 tunes, ATL-PHYS-PUB-2012-003 (2012), https://cds.cern.ch/record/1474107
82. A.D. Martin, W.J. Stirling, R.S. Thorne, G. Watt, Parton distributions for the LHC. Eur. Phys. J. C **63**, 189 (2009). arXiv:0901.0002 [hep-ph]
83. ATLAS Collaboration, Early Inner Detector Tracking Performance in the 2015 Data at $\sqrt{s} = 13$ TeV, ATL-PHYS-PUB-2015-051 (2015). https://cds.cern.ch/record/2110140

84. ATLAS Collaboration, Topological cell clustering in the ATLAS calorimeters and its performance in LHC Run 1. Eur. Phys. J. C **77**, 490 (2017). arXiv:1603.02934 [hep-ex]
85. M. Cacciari, G.P. Salam, G. Soyez, The anti-k_t jet clustering algorithm. JHEP **04**, 063 (2008). arXiv:0802.1189 [hep-ph]
86. M. Cacciari, G.P. Salam, G. Soyez, FastJet user manual. Eur. Phys. J. C **72**, 1896 (2012). arXiv:1111.6097 [hep-ph]
87. ATLAS Collaboration, Selection of jets produced in 13 TeV proton–proton collisions with the ATLAS detector, ATLAS-CONF-2015-029 (2015). https://cds.cern.ch/record/2037702
88. Y. Dokshitzer, G. Leder, S. Moretti, B. Webber, Better jet clustering algorithms. JHEP **08**, 001 (1997). arXiv:hep-ph/9707323 [hep-ph]
89. A. Hocker et al., TMVA—Toolkit for Multivariate Data Analysis (2007). arXiv:physics/0703039 [physics.data-an]
90. ATLAS Collaboration, The Level-1 Trigger Muon Barrel System of the ATLAS experiment at CERN, JINST 4, P04010 (2009)
91. ATLAS Collaboration, Tagging and suppression of pileup jets with the ATLAS detector, ATLASCONF-2014-018 (2014). https://cds.cern.ch/record/1700870
92. ATLAS Collaboration, Jet mass reconstruction with the ATLAS Detector in early Run 2 data, ATLAS-CONF-2016-035 (2016). https://cds.cern.ch/record/2200211
93. M. Cacciari, G.P. Salam, G. Soyez, The catchment area of jets. JHEP **04**, 005 (2008). arXiv:0802.1188 [hep-ph]
94. ATLAS Collaboration, Triggers for displaced decays of long-lived neutral particles in the ATLAS detector. JINST **8**, P07015 (2013). arXiv:1305.2284 [hep-ex]
95. ATLAS collaboration, Luminosity determination in pp collisions at $\sqrt{s} = 13$ TeV using the ATLAS detector at the LHC, ATLAS-CONF-2019-021 (2019). https://cds.cern.ch/record/2677054
96. G. Avoni et al., The new LUCID-2 detector for luminosity measurement and monitoring in ATLAS. JINST **13**, P07017 (2018)
97. ATLAS Collaboration, Search for long-lived neutral particles in pp collisions at $\sqrt{s} = 13$ TeV that decay into displaced hadronic jets in the ATLAS calorimeter. Eur. Phys. J. C **79**, 481 (2019). arXiv:1902.03094 [hep-ex]
98. ATLAS Collaboration, Jet energy scale measurements and their systematic uncertainties in proton–proton collisions at $\sqrt{s} = 13$ TeV with the ATLAS detector. Phys. Rev. D **96**, 072002 (2017). arXiv:1703.09665 [hep-ex]
99. A.L. Read, Presentation of search results: the CLs technique. J. Phys. G **28**, 2693 (2002)
100. ATLAS Collaboration, ATLAS Computing Acknowledgements, ATL-GEN-PUB-2016-002. https://cds.cern.ch/record/2202407

ATLAS Collaboration

G. Aad[102], B. Abbott[129], D. C. Abbott[103], A. Abed Abud[71a,71b], K. Abeling[53], D. K. Abhayasinghe[94], S. H. Abidi[167], O. S. AbouZeid[40], N. L. Abraham[156], H. Abramowicz[161], H. Abreu[160], Y. Abulaiti[6], B. S. Acharya[67a,67b,o], B. Achkar[53], S. Adachi[163], L. Adam[100], C. Adam Bourdarios[5], L. Adamczyk[84a], L. Adamek[167], J. Adelman[121], M. Adersberger[114], A. Adiguzel[12c,ak], S. Adorni[54], T. Adye[144], A. A. Affolder[146], Y. Afik[160], C. Agapopoulou[65], M. N. Agaras[38], A. Aggarwal[119], C. Agheorghiesei[27c], J. A. Aguilar-Saavedra[140f,140a,aj], F. Ahmadov[80], W. S. Ahmed[104], X. Ai[18], G. Aielli[74a,74b], S. Akatsuka[86], T. P. A. Åkesson[97], E. Akilli[54], A. V. Akimov[111], K. Al Khoury[65], G. L. Alberghi[23a,23b], J. Albert[176], M. J. Alconada Verzini[161], S. Alderweireldt[36], M. Aleksa[36], I. N. Aleksandrov[80], C. Alexa[27b], D. Alexandre[19], T. Alexopoulos[10], A. Alfonsi[120], M. Alhroob[129], B. Ali[142], G. Alimonti[69a], J. Alison[37], S. P. Alkire[148], C. Allaire[65], B. M. M. Allbrooke[156], B. W. Allen[132], P. P. Allport[21], A. Aloisio[70a,70b], A. Alonso[40], F. Alonso[89], C. Alpigiani[148], A. A. Alshehri[57], M. Alvarez Estevez[99], D. Álvarez Piqueras[174], M. G. Alviggi[70a,70b], Y. Amaral Coutinho[81b], A. Ambler[104], L. Ambroz[135], C. Amelung[26], D. Amidei[106], S. P. Amor Dos Santos[140a], S. Amoroso[46], C. S. Amrouche[54], F. An[79], C. Anastopoulos[149], N. Andari[145], T. Andeen[11], C. F. Anders[61b], J. K. Anders[20], A. Andreazza[69a,69b], V. Andrei[61a], C. R. Anelli[176], S. Angelidakis[38], A. Angerami[39], A. V. Anisenkov[122a,122b], A. Annovi[72a], C. Antel[61a], M. T. Anthony[149], M. Antonelli[51], D. J. A. Antrim[171], F. Anulli[73a], M. Aoki[82], J. A. Aparisi Pozo[174], L. Aperio Bella[36], G. Arabidze[107], J. P. Araque[140a], V. Araujo Ferraz[81b], R. Araujo Pereira[81b], C. Arcangeletti[51], A. T. H. Arce[49], F. A. Arduh[89], J -F. Arguin[110], S. Argyropoulos[78], J. -H. Arling[46], A. J. Armbruster[36], A. Armstrong[171], O. Arnaez[167], H. Arnold[120], A. Artamonov[124,*], G. Artoni[135], S. Artz[100], S. Asai[163], N. Asbah[59], E. M. Asimakopoulou[172], L. Asquith[156], J. Assahsah[35d], K. Assamagan[29], R. Astalos[28a], R. J. Atkin[33a], M. Atkinson[173], N. B. Atlay[19], H. Atmani[65], K. Augsten[142], G. Avolio[36], R. Avramidou[60a], M. K. Ayoub[15a], A. M. Azoulay[168b], G. Azuelos[110,ax], H. Bachacou[145], K. Bachas[68a,68b], M. Backes[135], F. Backman[45a,45b], P. Bagnaia[73a,73b], M. Bahmani[85], H. Bahrasemani[152], A. J. Bailey[174], V. R. Bailey[173], J. T. Baines[144], M. Bajic[40], C. Bakalis[10], O. K. Baker[183], P. J. Bakker[120], D. Bakshi Gupta[8], S. Balaji[157], E. M. Baldin[122a,122b], P. Balek[180], F. Balli[145], W. K. Balunas[135], J. Balz[100], E. Banas[85], A. Bandyopadhyay[24], Sw. Banerjee[181,j], A. A. E. Bannoura[182], L. Barak[161], W. M. Barbe[38], E. L. Barberio[105], D. Barberis[55a,55b], M. Barbero[102], T. Barillari[115], M -S. Barisits[36], J. Barkeloo[132], T. Barklow[153], R. Barnea[160], S. L. Barnes[60c], B. M. Barnett[144], R. M. Barnett[18], Z. Barnovska-Blenessy[60a], A. Baroncelli[60a], G. Barone[29], A. J. Barr[135], L. Barranco Navarro[45a,45b], F. Barreiro[99], J. Barreiro Guimarães da Costa[15a], S. Barsov[138], R. Bartoldus[153], G. Bartolini[102], A. E. Barton[90], P. Bartos[28a], A. Basalaev[46], A. Bassalat[65,ar], M. J. Basso[167], R. L. Bates[57], S. Batlamous[35e], J. R. Batley[32], B. Batool[151], M. Battaglia[146], M. Bauce[73a,73b], F. Bauer[145], K. T. Bauer[171], H. S. Bawa[31,m], J. B. Beacham[49], T. Beau[136], P. H. Beauchemin[170], F. Becherer[52], P. Bechtle[24], H. C. Beck[53], H. P. Beck[20,s], K. Becker[52], M. Becker[100], C. Becot[46], A. Beddall[12d], A. J. Beddall[12a], V. A. Bednyakov[80], M. Bedognetti[120], C. P. Bee[155], T. A. Beermann[77],

M. Begalli[81b], M. Begel[29], A. Behera[155], J. K. Behr[46], F. Beisiegel[24], A. S. Bell[95], G. Bella[161], L. Bellagamba[23b], A. Bellerive[34], P. Bellos[9], K. Beloborodov[122a,122b], K. Belotskiy[112], N. L. Belyaev[112], D. Benchekroun[35a], N. Benekos[10], Y. Benhammou[161], D. P. Benjamin[6], M. Benoit[54], J. R. Bensinger[26], S. Bentvelsen[120], L. Beresford[135], M. Beretta[51], D. Berge[46], E. Bergeaas Kuutmann[172], N. Berger[5], B. Bergmann[142], L. J. Bergsten[26], J. Beringer[18], S. Berlendis[7], N. R. Bernard[103], G. Bernardi[136], C. Bernius[153], F. U. Bernlochner[24], T. Berry[94], P. Berta[100], C. Bertella[15a], I. A. Bertram[90], O. Bessidskaia Bylund[182], N. Besson[145], A. Bethani[101], S. Bethke[115], A. Betti[24], A. J. Bevan[93], J. Beyer[115], R. Bi[139], R. M. Bianchi[139], O. Biebel[114], D. Biedermann[19], R. Bielski[36], K. Bierwagen[100], N. V. Biesuz[72a,72b], M. Biglietti[75a], T. R. V. Billoud[110], M. Bindi[53], A. Bingul[12d], C. Bini[73a,73b], S. Biondi[23a,23b], M. Birman[180], T. Bisanz[53], J. P. Biswal[161], D. Biswas[181,j], A. Bitadze[101], C. Bittrich[48], K. Bjørke[134], K. M. Black[25], T. Blazek[28a], I. Bloch[46], C. Blocker[26], A. Blue[57], U. Blumenschein[93], G. J. Bobbink[120], V. S. Bobrovnikov[122a,122b], S. S. Bocchetta[97], A. Bocci[49], D. Boerner[46], D. Bogavac[14], A. G. Bogdanchikov[122a,122b], C. Bohm[45a], V. Boisvert[94], P. Bokan[53,172], T. Bold[84a], A. S. Boldyrev[113], A. E. Bolz[61b], M. Bomben[136], M. Bona[93], J. S. Bonilla[132], M. Boonekamp[145], H. M. Borecka-Bielska[91], A. Borisov[123], G. Borissov[90], J. Bortfeldt[36], D. Bortoletto[135], V. Bortolotto[74a,74b], D. Boscherini[23b], M. Bosman[14], J. D. Bossio Sola[104], K. Bouaouda[35a], J. Boudreau[139], E. V. Bouhova-Thacker[90], D. Boumediene[38], S. K. Boutle[57], A. Boveia[127], J. Boyd[36], D. Boye[33c,as], I. R. Boyko[80], A. J. Bozson[94], J. Bracinik[21], N. Brahimi[102], G. Brandt[182], O. Brandt[32], F. Braren[46], B. Brau[103], J. E. Brau[132], W. D. Breaden Madden[57], K. Brendlinger[46], L. Brenner[46], R. Brenner[172], S. Bressler[180], B. Brickwedde[100], D. L. Briglin[21], D. Britton[57], D. Britzger[115], I. Brock[24], R. Brock[107], G. Brooijmans[39], W. K. Brooks[147d], E. Brost[121], J. H. Broughton[21], P. A. Bruckman de Renstrom[85], D. Bruncko[28b], A. Bruni[23b], G. Bruni[23b], L. S. Bruni[120], S. Bruno[74a,74b], B. H. Brunt[32], M. Bruschi[23b], N. Bruscino[139], P. Bryant[37], L. Bryngemark[97], T. Buanes[17], Q. Buat[36], P. Buchholz[151], A. G. Buckley[57], I. A. Budagov[80], M. K. Bugge[134], F. Bührer[52], O. Bulekov[112], T. J. Burch[121], S. Burdin[91], C. D. Burgard[120], A. M. Burger[130], B. Burghgrave[8], J. T. P. Burr[46], J. C. Burzynski[103], V. Büscher[100], E. Buschmann[53], P. J. Bussey[57], J. M. Butler[25], C. M. Buttar[57], J. M. Butterworth[95], P. Butti[36], W. Buttinger[36], A. Buzatu[158], A. R. Buzykaev[122a,122b], G. Cabras[23a,23b], S. Cabrera Urbán[174], D. Caforio[56], H. Cai[173], V. M. M. Cairo[153], O. Cakir[4a], N. Calace[36], P. Calafiura[18], A. Calandri[102], G. Calderini[136], P. Calfayan[66], G. Callea[57], L. P. Caloba[81b], S. Calvente Lopez[99], D. Calvet[38], S. Calvet[38], T. P. Calvet[155], M. Calvetti[72a,72b], R. Camacho Toro[136], S. Camarda[36], D. Camarero Munoz[99], P. Camarri[74a,74b], D. Cameron[134], R. Caminal Armadans[103], C. Camincher[36], S. Campana[36], M. Campanelli[95], A. Camplani[40], A. Campoverde[151], V. Canale[70a,70b], A. Canesse[104], M. Cano Bret[60c], J. Cantero[130], T. Cao[161], Y. Cao[173], M. D. M. Capeans Garrido[36], M. Capua[41a,41b], R. Cardarelli[74a], F. Cardillo[149], G. Carducci[41a,41b], I. Carli[143], T. Carli[36], G. Carlino[70a], B. T. Carlson[139], L. Carminati[69a,69b], R. M. D. Carney[45a,45b], S. Caron[119], E. Carquin[147d], S. Carrá[46], J. W. S. Carter[167], M. P. Casado[14,e], A. F. Casha[167], D. W. Casper[171], R. Castelijn[120], F. L. Castillo[174], V. Castillo Gimenez[174], N. F. Castro[140a,140e], A. Catinaccio[36], J. R. Catmore[134], A. Cattai[36], J. Caudron[24], V. Cavaliere[29], E. Cavallaro[14], M. Cavalli-Sforza[14], V. Cavasinni[72a,72b], E. Celebi[12b], F. Ceradini[75a,75b], L. Cerda Alberich[174], K. Cerny[131], A. S. Cerqueira[81a], A. Cerri[156], L. Cerrito[74a,74b], F. Cerutti[18], A. Cervelli[23a,23b], S. A. Cetin[12b], Z. Chadi[35a], D. Chakraborty[121], S. K. Chan[59], W. S. Chan[120], W. Y. Chan[91], J. D. Chapman[32], B. Chargeishvili[159b], D. G. Charlton[21], T. P. Charman[93], C. C. Chau[34], S. Che[127], A. Chegwidden[107], S. Chekanov[6], S. V. Chekulaev[168a], G. A. Chelkov[80], M. A. Chelstowska[36], B. Chen[79], C. Chen[60a], C. H. Chen[79], H. Chen[29], J. Chen[60a], J. Chen[39], S. Chen[137], S. J. Chen[15c], X. Chen[15b,aw], Y. Chen[83], Y -H. Chen[46], H. C. Cheng[63a], H. J. Cheng[15a], A. Cheplakov[80], E. Cheremushkina[123], R. Cherkaoui El Moursli[35e], E. Cheu[7], K. Cheung[64], T. J. A. Chevalérias[145], L. Chevalier[145], V. Chiarella[51], G. Chiarelli[72a], G. Chiodini[68a], A. S. Chisholm[36,21], A. Chitan[27b], I. Chiu[163], Y. H. Chiu[176], M. V. Chizhov[80], K. Choi[66], A. R. Chomont[73a,73b], S. Chouridou[162], Y. S. Chow[120], M. C. Chu[63a], X. Chu[15a,15d], J. Chudoba[141], A. J. Chuinard[104], J. J. Chwastowski[85], L. Chytka[131], D. Cieri[115], K. M. Ciesla[85], D. Cinca[47], V. Cindro[92], I. A. Cioară[27b], A. Ciocio[18], F. Cirotto[70a,70b], Z. H. Citron[180,k], M. Citterio[69a], D. A. Ciubotaru[27b], B. M. Ciungu[167], A. Clark[54], M. R. Clark[39], P. J. Clark[50], C. Clement[45a,45b], Y. Coadou[102], M. Cobal[67a,67c], A. Coccaro[55b], J. Cochran[79], H. Cohen[161], A. E. C. Coimbra[36], L. Colasurdo[119], B. Cole[39], A. P. Colijn[120], J. Collot[58], P. Conde Muiño[140a,f], E. Coniavitis[52], S. H. Connell[33c], I. A. Connelly[57], S. Constantinescu[27b], F. Conventi[70a,ay], A. M. Cooper-Sarkar[135], F. Cormier[175], K. J. R. Cormier[167], L. D. Corpe[95], M. Corradi[73a,73b], E. E. Corrigan[97], F. Corriveau[104,af], A. Cortes-Gonzalez[36], M. J. Costa[174], F. Costanza[5], D. Costanzo[149], G. Cowan[94], J. W. Cowley[32], J. Crane[101], K. Cranmer[125], S. J. Crawley[57], R. A. Creager[137], S. Crépé-Renaudin[58], F. Crescioli[136], M. Cristinziani[24], V. Croft[120], G. Crosetti[41a,41b], A. Cueto[5], T. Cuhadar Donszelmann[149], A. R. Cukierman[153], S. Czekierda[85], P. Czodrowski[36], M. J. Da Cunha Sargedas De Sousa[60b], J. V. Da Fonseca Pinto[81b], C. Da Via[101], W. Dabrowski[84a], T. Dado[28a], S. Dahbi[35e], T. Dai[106], C. Dallapiccola[103], M. Dam[40], G. D'amen[29], V. D'Amico[75a,75b], J. Damp[100], J. R. Dandoy[137], M. F. Daneri[30], N. P. Dang[181,j], N. S. Dann[101], M. Danninger[175], V. Dao[36], G. Darbo[55b], O. Dartsi[5], A. Dattagupta[132], T. Daubney[46], S. D'Auria[69a,69b], W. Davey[24], C. David[46], T. Davidek[143], D. R. Davis[49],

I. Dawson[149], K. De[8], R. De Asmundis[70a], M. De Beurs[120], S. De Castro[23a,23b], S. De Cecco[73a,73b], N. De Groot[119], P. de Jong[120], H. De la Torre[107], A. De Maria[15c], D. De Pedis[73a], A. De Salvo[73a], U. De Sanctis[74a,74b], M. De Santis[74a,74b], A. De Santo[156], K. De Vasconcelos Corga[102], J. B. De Vivie De Regie[65], C. Debenedetti[146], D. V. Dedovich[80], A. M. Deiana[42], M. Del Gaudio[41a,41b], J. Del Peso[99], Y. Delabat Diaz[46], D. Delgove[65], F. Deliot[145,r], C. M. Delitzsch[7], M. Della Pietra[70a,70b], D. Della Volpe[54], A. Dell'Acqua[36], L. Dell'Asta[74a,74b], M. Delmastro[5], C. Delporte[65], P. A. Delsart[58], D. A. DeMarco[167], S. Demers[183], M. Demichev[80], G. Demontigny[110], S. P. Denisov[123], D. Denysiuk[120], L. D'Eramo[136], D. Derendarz[85], J. E. Derkaoui[35d], F. Derue[136], P. Dervan[91], K. Desch[24], C. Deterre[46], K. Dette[167], C. Deutsch[24], M. R. Devesa[30], P. O. Deviveiros[36], A. Dewhurst[144], F. A. Di Bello[54], A. Di Ciaccio[74a,74b], L. Di Ciaccio[5], W. K. Di Clemente[137], C. Di Donato[70a,70b], A. Di Girolamo[36], G. Di Gregorio[72a,72b], B. Di Micco[75a,75b], R. Di Nardo[103], K. F. Di Petrillo[59], R. Di Sipio[167], D. Di Valentino[34], C. Diaconu[102], F. A. Dias[40], T. Dias Do Vale[140a], M. A. Diaz[147a], J. Dickinson[18], E. B. Diehl[106], J. Dietrich[19], S. Díez Cornell[46], A. Dimitrievska[18], W. Ding[15b], J. Dingfelder[24], F. Dittus[36], F. Djama[102], T. Djobava[159b], J. I. Djuvsland[17], M. A. B. Do Vale[81c], M. Dobre[27b], D. Dodsworth[26], C. Doglioni[97], J. Dolejsi[143], Z. Dolezal[143], M. Donadelli[81d], B. Dong[60c], J. Donini[38], A. D'onofrio[93], M. D'Onofrio[91], J. Dopke[144], A. Doria[70a], M. T. Dova[89], A. T. Doyle[57], E. Drechsler[152], E. Dreyer[152], T. Dreyer[53], A. S. Drobac[170], Y. Duan[60b], F. Dubinin[111], M. Dubovsky[28a], A. Dubreuil[54], E. Duchovni[180], G. Duckeck[114], A. Ducourthial[136], O. A. Ducu[110], D. Duda[115], A. Dudarev[36], A. C. Dudder[100], E. M. Duffield[18], L. Duflot[65], M. Dührssen[36], C. Dülsen[182], M. Dumancic[180], A. E. Dumitriu[27b], A. K. Duncan[57], M. Dunford[61a], A. Duperrin[102], H. Duran Yildiz[4a], M. Düren[56], A. Durglishvili[159b], D. Duschinger[48], B. Dutta[46], D. Duvnjak[1], G. I. Dyckes[137], M. Dyndal[36], S. Dysch[101], B. S. Dziedzic[85], K. M. Ecker[115], R. C. Edgar[106], M. G. Eggleston[49], T. Eifert[36], G. Eigen[17], K. Einsweiler[18], T. Ekelof[172], H. El Jarrari[35e], M. El Kacimi[35c], R. El Kosseifi[102], V. Ellajosyula[172], M. Ellert[172], F. Ellinghaus[182], A. A. Elliot[93], N. Ellis[36], J. Elmsheuser[29], M. Elsing[36], D. Emeliyanov[144], A. Emerman[39], Y. Enari[163], M. B. Epland[49], J. Erdmann[47], A. Ereditato[20], M. Errenst[36], M. Escalier[65], C. Escobar[174], O. Estrada Pastor[174], E. Etzion[161], H. Evans[66], A. Ezhilov[138], F. Fabbri[57], L. Fabbri[23a,23b], V. Fabiani[119], G. Facini[95], R. M. Faisca Rodrigues Pereira[140a], R. M. Fakhrutdinov[123], S. Falciano[73a], P. J. Falke[5], S. Falke[5], J. Faltova[143], Y. Fang[15a], Y. Fang[15a], G. Fanourakis[44], M. Fanti[69a,69b], M. Faraj[67a,67c,u], A. Farbin[8], A. Farilla[75a], E. M. Farina[71a,71b], T. Farooque[107], S. Farrell[18], S. M. Farrington[50], P. Farthouat[36], F. Fassi[35e], P. Fassnacht[36], D. Fassouliotis[9], M. Faucci Giannelli[50], W. J. Fawcett[32], L. Fayard[65], O. L. Fedin[138,p], W. Fedorko[175], M. Feickert[42], L. Feligioni[102], A. Fell[149], C. Feng[60b], E. J. Feng[36], M. Feng[49], M. J. Fenton[57], A. B. Fenyuk[123], J. Ferrando[46], A. Ferrante[173], A. Ferrari[172], P. Ferrari[120], R. Ferrari[71a], D. E. Ferreira de Lima[61b], A. Ferrer[174], D. Ferrere[54], C. Ferretti[106], F. Fiedler[100], A. Filipčič[92], F. Filthaut[119], K. D. Finelli[25], M. C. N. Fiolhais[140a,140c,a], L. Fiorini[174], F. Fischer[114], W. C. Fisher[107], I. Fleck[151], P. Fleischmann[106], R. R. M. Fletcher[137], T. Flick[182], B. M. Flierl[114], L. Flores[137], L. R. Flores Castillo[63a], F. M. Follega[76a,76b], N. Fomin[17], J. H. Foo[167], G. T. Forcolin[76a,76b], A. Formica[145], F. A. Förster[14], A. C. Forti[101], A. G. Foster[21], M. G. Foti[135], D. Fournier[65], H. Fox[90], P. Francavilla[72a,72b], S. Francescato[73a,73b], M. Franchini[23a,23b], S. Franchino[61a], D. Francis[36], L. Franconi[20], M. Franklin[59], A. N. Fray[93], P. M. Freeman[21], B. Freund[110], W. S. Freund[81b], E. M. Freundlich[47], D. C. Frizzell[129], D. Froidevaux[36], J. A. Frost[135], C. Fukunaga[164], E. Fullana Torregrosa[174], E. Fumagalli[55a,55b], T. Fusayasu[116], J. Fuster[174], A. Gabrielli[23a,23b], A. Gabrielli[18], G. P. Gach[84a], S. Gadatsch[54], P. Gadow[115], G. Gagliardi[55a,55b], L. G. Gagnon[110], C. Galea[27b], B. Galhardo[140a], G. E. Gallardo[135], E. J. Gallas[135], B. J. Gallop[144], G. Galster[40], R. Gamboa Goni[93], K. K. Gan[127], S. Ganguly[180], J. Gao[60a], Y. Gao[50], Y. S. Gao[31,m], C. García[174], J. E. García Navarro[174], J. A. García Pascual[15a], C. Garcia-Argos[52], M. Garcia-Sciveres[18], R. W. Gardner[37], N. Garelli[153], S. Gargiulo[52], V. Garonne[134], A. Gaudiello[55a,55b], G. Gaudio[71a], I. L. Gavrilenko[111], A. Gavrilyuk[124], C. Gay[175], G. Gaycken[46], E. N. Gazis[10], A. A. Geanta[27b], C. N. P. Gee[144], J. Geisen[53], M. Geisen[100], M. P. Geisler[61a], C. Gemme[55b], M. H. Genest[58], C. Geng[106], S. Gentile[73a,73b], S. George[94], T. Geralis[44], L. O. Gerlach[53], P. Gessinger-Befurt[100], G. Gessner[47], S. Ghasemi[151], M. Ghasemi Bostanabad[176], A. Ghosh[65], A. Ghosh[78], B. Giacobbe[23b], S. Giagu[73a,73b], N. Giangiacomi[23a,23b], P. Giannetti[72a], A. Giannini[70a,70b], G. Giannini[14], S. M. Gibson[94], M. Gignac[146], D. Gillberg[34], G. Gilles[182], D. M. Gingrich[3,ax], M. P. Giordani[67a,67c], F. M. Giorgi[23b], P. F. Giraud[145], G. Giugliarelli[67a,67c], D. Giugni[69a], F. Giuli[74a,74b], S. Gkaitatzis[162], I. Gkialas[9,h], E. L. Gkougkousis[14], P. Gkountoumis[10], L. K. Gladilin[113], C. Glasman[99], J. Glatzer[14], P. C. F. Glaysher[46], A. Glazov[46], G. R. Gledhill[132], M. Goblirsch-Kolb[26], S. Goldfarb[105], T. Golling[54], D. Golubkov[123], A. Gomes[140a,140b], R. Goncalves Gama[53], R. Gonçalo[140a], G. Gonella[52], L. Gonella[21], A. Gongadze[80], F. Gonnella[21], J. L. Gonski[59], S. González de la Hoz[174], S. Gonzalez-Sevilla[54], G. R. Gonzalvo Rodriguez[174], L. Goossens[36], P. A. Gorbounov[124], H. A. Gordon[29], B. Gorini[36], E. Gorini[68a,68b], A. Gorišek[92], A. T. Goshaw[49], M. I. Gostkin[80], C. A. Gottardo[119], M. Gouighri[35b], D. Goujdami[35c], A. G. Goussiou[148], N. Govender[33c], C. Goy[5], E. Gozani[160], I. Grabowska-Bold[84a], E. C. Graham[91], J. Gramling[171], E. Gramstad[134], S. Grancagnolo[19], M. Grandi[156], V. Gratchev[138], P. M. Gravila[27f], F. G. Gravili[68a,68b], C. Gray[57], H. M. Gray[18], C. Grefe[24], K. Gregersen[97], I. M. Gregor[46], P. Grenier[153], K. Grevtsov[46],

C. Grieco[14], N. A. Grieser[129], J. Griffiths[8], A. A. Grillo[146], K. Grimm[31,l], S. Grinstein[14,aa], J. -F. Grivaz[65], S. Groh[100], E. Gross[180], J. Grosse-Knetter[53], Z. J. Grout[95], C. Grud[106], A. Grummer[118], L. Guan[106], W. Guan[181], J. Guenther[36], A. Guerguichon[65], J. G. R. Guerrero Rojas[174], F. Guescini[115], D. Guest[171], R. Gugel[52], T. Guillemin[5], S. Guindon[36], U. Gul[57], J. Guo[60c], W. Guo[106], Y. Guo[60a,t], Z. Guo[102], R. Gupta[46], S. Gurbuz[12c], G. Gustavino[129], P. Gutierrez[129], C. Gutschow[95], C. Guyot[145], C. Gwenlan[135], C. B. Gwilliam[91], A. Haas[125], C. Haber[18], H. K. Hadavand[8], N. Haddad[35e], A. Hadef[60a], S. Hageböck[36], M. Haleem[177], J. Haley[130], G. Halladjian[107], G. D. Hallewell[102], K. Hamacher[182], P. Hamal[131], K. Hamano[176], H. Hamdaoui[35e], G. N. Hamity[149], K. Han[60a,z], L. Han[60a], S. Han[15a], Y. F. Han[167], K. Hanagaki[82,x], M. Hance[146], D. M. Handl[114], B. Haney[137], R. Hankache[136], E. Hansen[97], J. B. Hansen[40], J. D. Hansen[40], M. C. Hansen[24], P. H. Hansen[40], E. C. Hanson[101], K. Hara[169], A. S. Hard[181], T. Harenberg[182], S. Harkusha[108], P. F. Harrison[178], N. M. Hartmann[114], Y. Hasegawa[150], A. Hasib[50], S. Hassani[145], S. Haug[20], R. Hauser[107], L. B. Havener[39], M. Havranek[142], C. M. Hawkes[21], R. J. Hawkings[36], D. Hayden[107], C. Hayes[155], R. L. Hayes[175], C. P. Hays[135], J. M. Hays[93], H. S. Hayward[91], S. J. Haywood[144], F. He[60a], M. P. Heath[50], V. Hedberg[97], L. Heelan[8], S. Heer[24], K. K. Heidegger[52], W. D. Heidorn[79], J. Heilman[34], S. Heim[46], T. Heim[18], B. Heinemann[46,at], J. J. Heinrich[132], L. Heinrich[36], C. Heinz[56], J. Hejbal[141], L. Helary[61b], A. Held[175], S. Hellesund[134], C. M. Helling[146], S. Hellman[45a,45b], C. Helsens[36], R. C. W. Henderson[90], Y. Heng[181], S. Henkelmann[175], A. M. Henriques Correia[36], G. H. Herbert[19], H. Herde[26], V. Herget[177], Y. Hernández Jiménez[33e], H. Herr[100], M. G. Herrmann[114], T. Herrmann[48], G. Herten[52], R. Hertenberger[114], L. Hervas[36], T. C. Herwig[137], G. G. Hesketh[95], N. P. Hessey[168a], A. Higashida[163], S. Higashino[82], E. Higón-Rodriguez[174], K. Hildebrand[37], E. Hill[176], J. C. Hill[32], K. K. Hill[29], K. H. Hiller[46], S. J. Hillier[21], M. Hils[48], I. Hinchliffe[18], F. Hinterkeuser[24], M. Hirose[133], S. Hirose[52], D. Hirschbuehl[182], B. Hiti[92], O. Hladik[141], D. R. Hlaluku[33e], X. Hoad[50], J. Hobbs[155], N. Hod[180], M. C. Hodgkinson[149], A. Hoecker[36], F. Hoenig[114], D. Hohn[52], D. Hohov[65], T. R. Holmes[37], M. Holzbock[114], L. B. A. H. Hommels[32], S. Honda[169], T. M. Hong[139], A. Hönle[115], B. H. Hooberman[173], W. H. Hopkins[6], Y. Horii[117], P. Horn[48], L. A. Horyn[37], S. Hou[158], A. Hoummada[35a], J. Howarth[101], J. Hoya[89], M. Hrabovsky[131], J. Hrdinka[77], I. Hristova[19], J. Hrivnac[65], A. Hrynevich[109], T. Hryn'ova[5], P. J. Hsu[64], S. -C. Hsu[148], Q. Hu[29], S. Hu[60c], D. P. Huang[95], Y. Huang[60a], Y. Huang[15a], Z. Hubacek[142], F. Hubaut[102], M. Huebner[24], F. Huegging[24], T. B. Huffman[135], M. Huhtinen[36], R. F. H. Hunter[34], P. Huo[155], A. M. Hupe[34], N. Huseynov[80,ah], J. Huston[107], J. Huth[59], R. Hyneman[106], S. Hyrych[28a], G. Iacobucci[54], G. Iakovidis[29], I. Ibragimov[151], L. Iconomidou-Fayard[65], Z. Idrissi[35e], P. Iengo[36], R. Ignazzi[40], O. Igonkina[120,ac,*], R. Iguchi[163], T. Iizawa[54], Y. Ikegami[82], M. Ikeno[82], D. Iliadis[162], N. Ilic[119,167,af], F. Iltzsche[48], G. Introzzi[71a,71b], M. Iodice[75a], K. Iordanidou[168a], V. Ippolito[73a,73b], M. F. Isacson[172], M. Ishino[163], W. Islam[130], C. Issever[135], S. Istin[160], F. Ito[169], J. M. Iturbe Ponce[63a], R. Iuppa[76a,76b], A. Ivina[180], H. Iwasaki[82], J. M. Izen[43], V. Izzo[70a], P. Jacka[141], P. Jackson[1], R. M. Jacobs[24], B. P. Jaeger[152], V. Jain[2], G. Jäkel[182], K. B. Jakobi[100], K. Jakobs[52], S. Jakobsen[77], T. Jakoubek[141], J. Jamieson[57], K. W. Janas[84a], R. Jansky[54], J. Janssen[24], M. Janus[53], P. A. Janus[84a], G. Jarlskog[97], N. Javadov[80,ah], T. Javůrek[36], M. Javurkova[52], F. Jeanneau[145], L. Jeanty[132], J. Jejelava[159a,ai], A. Jelinskas[178], P. Jenni[52,b], J. Jeong[46], N. Jeong[46], S. Jézéquel[5], H. Ji[181], J. Jia[155], H. Jiang[79], Y. Jiang[60a], Z. Jiang[153,q], S. Jiggins[52], F. A. Jimenez Morales[38], J. Jimenez Pena[115], S. Jin[15c], A. Jinaru[27b], O. Jinnouchi[165], H. Jivan[33e], P. Johansson[149], K. A. Johns[7], C. A. Johnson[66], K. Jon-And[45a,45b], R. W. L. Jones[90], S. D. Jones[156], S. Jones[7], T. J. Jones[91], J. Jongmanns[61a], P. M. Jorge[140a], J. Jovicevic[36], X. Ju[18], J. J. Junggeburth[115], A. Juste Rozas[14,aa], A. Kaczmarska[85], M. Kado[73a,73b], H. Kagan[127], M. Kagan[153], C. Kahra[100], T. Kaji[179], E. Kajomovitz[160], C. W. Kalderon[97], A. Kaluza[100], A. Kamenshchikov[123], L. Kanjir[92], Y. Kano[163], V. A. Kantserov[112], J. Kanzaki[82], L. S. Kaplan[181], D. Kar[33e], K. Karava[135], M. J. Kareem[168b], S. N. Karpov[80], Z. M. Karpova[80], V. Kartvelishvili[90], A. N. Karyukhin[123], L. Kashif[181], R. D. Kass[127], A. Kastanas[45a,45b], C. Kato[60d,60c], J. Katzy[46], K. Kawade[150], K. Kawagoe[88], T. Kawaguchi[117], T. Kawamoto[163], G. Kawamura[53], E. F. Kay[176], V. F. Kazanin[122a,122b], R. Keeler[176], R. Kehoe[42], J. S. Keller[34], E. Kellermann[97], D. Kelsey[156], J. J. Kempster[21], J. Kendrick[21], O. Kepka[141], S. Kersten[182], B. P. Kerševan[92], S. Ketabchi Haghighat[167], M. Khader[173], F. Khalil-Zada[13], M. Khandoga[145], A. Khanov[130], A. G. Kharlamov[122a,122b], T. Kharlamova[122a,122b], E. E. Khoda[175], A. Khodinov[166], T. J. Khoo[54], E. Khramov[80], J. Khubua[159b], S. Kido[83], M. Kiehn[54], C. R. Kilby[94], Y. K. Kim[37], N. Kimura[95], O. M. Kind[19], B. T. King[91,*], D. Kirchmeier[48], J. Kirk[144], A. E. Kiryunin[115], T. Kishimoto[163], D. P. Kisliuk[167], V. Kitali[46], O. Kivernyk[5], T. Klapdor-Kleingrothaus[52], M. Klassen[61a], M. H. Klein[106], M. Klein[91], U. Klein[91], K. Kleinknecht[100], P. Klimek[121], A. Klimentov[29], T. Klingl[24], T. Klioutchnikova[36], F. F. Klitzner[114], P. Kluit[120], S. Kluth[115], E. Kneringer[77], E. B. F. G. Knoops[102], A. Knue[52], D. Kobayashi[88], T. Kobayashi[163], M. Kobel[48], M. Kocian[153], P. Kodys[143], P. T. Koenig[24], T. Koffas[34], N. M. Köhler[36], T. Koi[153], M. Kolb[61b], I. Koletsou[5], T. Komarek[131], T. Kondo[82], N. Kondrashova[60c], K. Köneke[52], A. C. König[119], T. Kono[126], R. Konoplich[125,ao], V. Konstantinides[95], N. Konstantinidis[95], B. Konya[97], R. Kopeliansky[66], S. Koperny[84a], K. Korcyl[85], K. Kordas[162], G. Koren[161], A. Korn[95], I. Korolkov[14], E. V. Korolkova[149], N. Korotkova[113], O. Kortner[115], S. Kortner[115], T. Kosek[143], V. V. Kostyukhin[166], A. Kotwal[49], A. Koulouris[10], A. Kourkoumeli-Charalampidi[71a,71b], C. Kourkoumelis[9], E. Kourlitis[149], V. Kouskoura[29],

A. B. Kowalewska[85], R. Kowalewski[176], C. Kozakai[163], W. Kozanecki[145], A. S. Kozhin[123], V. A. Kramarenko[113], G. Kramberger[92], D. Krasnopevtsev[60a], M. W. Krasny[136], A. Krasznahorkay[36], D. Krauss[115], J. A. Kremer[84a], J. Kretzschmar[91], P. Krieger[167], F. Krieter[114], A. Krishnan[61b], K. Krizka[18], K. Kroeninger[47], H. Kroha[115], J. Kroll[141], J. Kroll[137], J. Krstic[16], U. Kruchonak[80], H. Krüger[24], N. Krumnack[79], M. C. Kruse[49], J. A. Krzysiak[85], T. Kubota[105], O. Kuchinskaia[166], S. Kuday[4b], J. T. Kuechler[46], S. Kuehn[36], A. Kugel[61a], T. Kuhl[46], V. Kukhtin[80], R. Kukla[102], Y. Kulchitsky[108,al], S. Kuleshov[147d], Y. P. Kulinich[173], M. Kuna[58], T. Kunigo[86], A. Kupco[141], T. Kupfer[47], O. Kuprash[52], H. Kurashige[83], L. L. Kurchaninov[168a], Y. A. Kurochkin[108], A. Kurova[112], M. G. Kurth[15a,15d], E. S. Kuwertz[36], M. Kuze[165], A. K. Kvam[148], J. Kvita[131], T. Kwan[104], A. La Rosa[115], L. La Rotonda[41a,41b], F. La Ruffa[41a,41b], C. Lacasta[174], F. Lacava[73a,73b], D. P. J. Lack[101], H. Lacker[19], D. Lacour[136], E. Ladygin[80], R. Lafaye[5], B. Laforge[136], T. Lagouri[33e], S. Lai[53], S. Lammers[66], W. Lampl[7], C. Lampoudis[162], E. Lançon[29], U. Landgraf[52], M. P. J. Landon[93], M. C. Lanfermann[54], V. S. Lang[46], J. C. Lange[53], R. J. Langenberg[36], A. J. Lankford[171], F. Lanni[29], K. Lantzsch[24], A. Lanza[71a], A. Lapertosa[55a,55b], S. Laplace[136], J. F. Laporte[145], T. Lari[69a], F. Lasagni Manghi[23a,23b], M. Lassnig[36], T. S. Lau[63a], A. Laudrain[65], A. Laurier[34], M. Lavorgna[70a,70b], M. Lazzaroni[69a,69b], B. Le[105], E. Le Guirriec[102], M. LeBlanc[7], T. LeCompte[6], F. Ledroit-Guillon[58], C. A. Lee[29], G. R. Lee[17], L. Lee[59], S. C. Lee[158], S. J. Lee[34], B. Lefebvre[168a], M. Lefebvre[176], F. Legger[114], C. Leggett[18], K. Lehmann[152], N. Lehmann[182], G. Lehmann Miotto[36], W. A. Leight[46], A. Leisos[162,y], M. A. L. Leite[81d], C. E. Leitgeb[114], R. Leitner[143], D. Lellouch[180,*], K. J. C. Leney[42], T. Lenz[24], B. Lenzi[36], R. Leone[7], S. Leone[72a], C. Leonidopoulos[50], A. Leopold[136], G. Lerner[156], C. Leroy[110], R. Les[167], C. G. Lester[32], M. Levchenko[138], J. Levêque[5], D. Levin[106], L. J. Levinson[180], D. J. Lewis[21], B. Li[15b], B. Li[106], C -Q. Li[60a], F. Li[60c], H. Li[60a], H. Li[60b], J. Li[60c], K. Li[153], L. Li[60c], M. Li[15a,15d], Q. Li[15a,15d], Q. Y. Li[60a], S. Li[60d,60c], X. Li[46], Y. Li[46], Z. Li[60b], Z. Liang[15a], B. Liberti[74a], A. Liblong[167], K. Lie[63c], S. Liem[120], C. Y. Lin[32], K. Lin[107], T. H. Lin[100], R. A. Linck[66], J. H. Lindon[21], A. L. Lionti[54], E. Lipeles[137], A. Lipniacka[17], M. Lisovyi[61b], T. M. Liss[173,av], A. Lister[175], A. M. Litke[146], J. D. Little[8], B. Liu[79], B. L. Liu[6], H. B. Liu[29], H. Liu[106], J. B. Liu[60a], J. K. K. Liu[135], K. Liu[136], M. Liu[60a], P. Liu[18], Y. Liu[15a,15d], Y. L. Liu[106], Y. W. Liu[60a], M. Livan[71a,71b], A. Lleres[58], J. Llorente Merino[152], S. L. Lloyd[93], C. Y. Lo[63b], F. Lo Sterzo[42], E. M. Lobodzinska[46], P. Loch[7], S. Loffredo[74a,74b], T. Lohse[19], K. Lohwasser[149], M. Lokajicek[141], J. D. Long[173], R. E. Long[90], L. Longo[36], K. A. Looper[127], J. A. Lopez[147d], I. Lopez Paz[101], A. Lopez Solis[149], J. Lorenz[114], N. Lorenzo Martinez[5], M. Losada[22a], P. J. Lösel[114], A. Lösle[52], X. Lou[46], X. Lou[15a], A. Lounis[65], J. Love[6], P. A. Love[90], J. J. Lozano Bahilo[174], M. Lu[60a], Y. J. Lu[64], H. J. Lubatti[148], C. Luci[73a,73b], A. Lucotte[58], C. Luedtke[52], F. Luehring[66], I. Luise[136], L. Luminari[73a], B. Lund-Jensen[154], M. S. Lutz[103], D. Lynn[29], R. Lysak[141], E. Lytken[97], F. Lyu[15a], V. Lyubushkin[80], T. Lyubushkina[80], H. Ma[29], L. L. Ma[60b], Y. Ma[60b], G. Maccarrone[51], A. Macchiolo[115], C. M. Macdonald[149], J. Machado Miguens[137], D. Madaffari[174], R. Madar[38], W. F. Mader[48], N. Madysa[48], J. Maeda[83], S. Maeland[17], T. Maeno[29], M. Maerker[48], A. S. Maevskiy[113], V. Magerl[52], N. Magini[79], D. J. Mahon[39], C. Maidantchik[81b], T. Maier[114], A. Maio[140a,140b,140d], K. Maj[84a], O. Majersky[28a], S. Majewski[132], Y. Makida[82], N. Makovec[65], B. Malaescu[136], Pa. Malecki[85], V. P. Maleev[138], F. Malek[58], U. Mallik[78], D. Malon[6], C. Malone[32], S. Maltezos[10], S. Malyukov[80], J. Mamuzic[174], G. Mancini[51], I. Mandić[92], L. Manhaes de Andrade Filho[81a], I. M. Maniatis[162], J. Manjarres Ramos[48], K. H. Mankinen[97], A. Mann[114], A. Manousos[77], B. Mansoulie[145], I. Manthos[162], S. Manzoni[120], A. Marantis[162], G. Marceca[30], L. Marchese[135], G. Marchiori[136], M. Marcisovsky[141], C. Marcon[97], C. A. Marin Tobon[36], M. Marjanovic[38], Z. Marshall[18], M. U. F. Martensson[172], S. Marti-Garcia[174], C. B. Martin[127], T. A. Martin[178], V. J. Martin[50], B. Martin dit Latour[17], L. Martinelli[75a,75b], M. Martinez[14,aa], V. I. Martinez Outschoorn[103], S. Martin-Haugh[144], V. S. Martoiu[27b], A. C. Martyniuk[95], A. Marzin[36], S. R. Maschek[115], L. Masetti[100], T. Mashimo[163], R. Mashinistov[111], J. Masik[101], A. L. Maslennikov[122a,122b], L. Massa[74a,74b], P. Massarotti[70a,70b], P. Mastrandrea[72a,72b], A. Mastroberardino[41a,41b], T. Masubuchi[163], D. Matakias[10], A. Matic[114], P. Mättig[24], J. Maurer[27b], B. Maček[92], D. A. Maximov[122a,122b], R. Mazini[158], I. Maznas[162], S. M. Mazza[146], S. P. Mc Kee[106], T. G. McCarthy[115], W. P. McCormack[18], E. F. McDonald[105], J. A. Mcfayden[36], M. A. McKay[42], K. D. McLean[176], S. J. McMahon[144], P. C. McNamara[105], C. J. McNicol[178], R. A. McPherson[176,af], J. E. Mdhluli[33e], Z. A. Meadows[103], S. Meehan[36], T. Megy[52], S. Mehlhase[114], A. Mehta[91], T. Meideck[58], B. Meirose[43], D. Melini[174], B. R. Mellado Garcia[33e], J. D. Mellenthin[53], M. Melo[28a], F. Meloni[46], A. Melzer[24], S. B. Menary[101], E. D. Mendes Gouveia[140a,140e], L. Meng[36], X. T. Meng[106], S. Menke[115], E. Meoni[41a,41b], S. Mergelmeyer[19], S. A. M. Merkt[139], C. Merlassino[20], P. Mermod[54], L. Merola[70a,70b], C. Meroni[69a], O. Meshkov[111,113], J. K. R. Meshreki[151], A. Messina[73a,73b], J. Metcalfe[6], A. S. Mete[171], C. Meyer[66], J. Meyer[160], J -P. Meyer[145], H. Meyer Zu Theenhausen[61a], F. Miano[156], M. Michetti[19], R. P. Middleton[144], L. Mijović[50], G. Mikenberg[180], M. Mikestikova[141], M. Mikuž[92], H. Mildner[149], M. Milesi[105], A. Milic[167], D. A. Millar[93], D. W. Miller[37], A. Milov[180], D. A. Milstead[45a,45b], R. A. Mina[153,q], A. A. Minaenko[123], M. Miñano Moya[174], I. A. Minashvili[159b], A. I. Mincer[125], B. Mindur[84a], M. Mineev[80], Y. Minegishi[163], Y. Ming[181], L. M. Mir[14], A. Mirto[68a,68b], K. P. Mistry[137], T. Mitani[179], J. Mitrevski[114], V. A. Mitsou[174], M. Mittal[60c], O. Miu[167], A. Miucci[20], P. S. Miyagawa[149], A. Mizukami[82],

J. U. Mjörnmark[97], T. Mkrtchyan[184], M. Mlynarikova[143], T. Moa[45a,45b], K. Mochizuki[110], P. Mogg[52], S. Mohapatra[39], R. Moles-Valls[24], M. C. Mondragon[107], K. Mönig[46], J. Monk[40], E. Monnier[102], A. Montalbano[152], J. Montejo Berlingen[36], M. Montella[95], F. Monticelli[89], S. Monzani[69a], N. Morange[65], D. Moreno[22a], M. Moreno Llácer[36], C. Moreno Martinez[14], P. Morettini[55b], M. Morgenstern[120], S. Morgenstern[48], D. Mori[152], M. Morii[59], M. Morinaga[179], V. Morisbak[134], A. K. Morley[36], G. Mornacchi[36], A. P. Morris[95], L. Morvaj[155], P. Moschovakos[36], B. Moser[120], M. Mosidze[159b], T. Moskalets[145], H. J. Moss[149], J. Moss[31,n], E. J. W. Moyse[103], S. Muanza[102], J. Mueller[139], R. S. P. Mueller[114], D. Muenstermann[90], G. A. Mullier[97], J. L. Munoz Martinez[14], F. J. Munoz Sanchez[101], P. Murin[28b], W. J. Murray[144,178], A. Murrone[69a,69b], M. Muškinja[18], C. Mwewa[33a], A. G. Myagkov[123,ap], J. Myers[132], M. Myska[142], B. P. Nachman[18], O. Nackenhorst[47], A.Nag Nag[48], K. Nagai[135], K. Nagano[82], Y. Nagasaka[62], M. Nagel[52], E. Nagy[102], A. M. Nairz[36], Y. Nakahama[117], K. Nakamura[82], T. Nakamura[163], I. Nakano[128], H. Nanjo[133], F. Napolitano[61a], R. F. Naranjo Garcia[46], R. Narayan[42], I. Naryshkin[138], T. Naumann[46], G. Navarro[22a], H. A. Neal[106,*], P. Y. Nechaeva[111], F. Nechansky[46], T. J. Neep[21], A. Negri[71a,71b], M. Negrini[23b], C. Nellist[53], M. E. Nelson[135], S. Nemecek[141], P. Nemethy[125], M. Nessi[36,d], M. S. Neubauer[173], M. Neumann[182], P. R. Newman[21], Y. S. Ng[19], Y. W. Y. Ng[171], B. Ngair[35e], H. D. N. Nguyen[102], T. Nguyen Manh[110], E. Nibigira[38], R. B. Nickerson[135], R. Nicolaidou[145], D. S. Nielsen[40], J. Nielsen[146], N. Nikiforou[11], V. Nikolaenko[123,ap], I. Nikolic-Audit[136], K. Nikolopoulos[21], P. Nilsson[29], H. R. Nindhito[54], Y. Ninomiya[82], A. Nisati[73a], N. Nishu[60c], R. Nisius[115], I. Nitsche[47], T. Nitta[179], T. Nobe[163], Y. Noguchi[86], I. Nomidis[136], M. A. Nomura[29], M. Nordberg[36], N. Norjoharuddeen[135], T. Novak[92], O. Novgorodova[48], R. Novotny[142], L. Nozka[131], K. Ntekas[171], E. Nurse[95], F. G. Oakham[34,ax], H. Oberlack[115], J. Ocariz[136], A. Ochi[83], I. Ochoa[39], J. P. Ochoa-Ricoux[147a], K. O'Connor[26], S. Oda[88], S. Odaka[82], S. Oerdek[53], A. Ogrodnik[84a], A. Oh[101], S. H. Oh[49], C. C. Ohm[154], H. Oide[165], M. L. Ojeda[167], H. Okawa[169], Y. Okazaki[86], Y. Okumura[163], T. Okuyama[82], A. Olariu[27b], L. F. Oleiro Seabra[140a], S. A. Olivares Pino[147a], D. Oliveira Damazio[29], J. L. Oliver[1], M. J. R. Olsson[171], A. Olszewski[85], J. Olszowska[85], D. C. O'Neil[152], A. P. O'neill[135], A. Onofre[140a,140e], P. U. E. Onyisi[11], H. Oppen[134], M. J. Oreglia[37], G. E. Orellana[89], D. Orestano[75a,75b], N. Orlando[14], R. S. Orr[167], V. O'Shea[57], R. Ospanov[60a], G. Otero y Garzon[30], H. Otono[88], P. S. Ott[61a], M. Ouchrif[35d], J. Ouellette[29], F. Ould-Saada[134], A. Ouraou[145], Q. Ouyang[15a], M. Owen[57], R. E. Owen[21], V. E. Ozcan[12c], N. Ozturk[8], J. Pacalt[131], H. A. Pacey[32], K. Pachal[49], A. Pacheco Pages[14], C. Padilla Aranda[14], S. Pagan Griso[18], M. Paganini[183], G. Palacino[66], S. Palazzo[50], S. Palestini[36], M. Palka[84b], D. Pallin[38], I. Panagoulias[10], C. E. Pandini[36], J. G. Panduro Vazquez[94], P. Pani[46], G. Panizzo[67a,67c], L. Paolozzi[54], C. Papadatos[110], K. Papageorgiou[9,h], S. Parajuli[43], A. Paramonov[6], D. Paredes Hernandez[63b], S. R. Paredes Saenz[135], B. Parida[166], T. H. Park[167], A. J. Parker[90], M. A. Parker[32], F. Parodi[55a,55b], E. W. Parrish[121], J. A. Parsons[39], U. Parzefall[52], L. Pascual Dominguez[136], V. R. Pascuzzi[167], J. M. P. Pasner[146], E. Pasqualucci[73a], S. Passaggio[55b], F. Pastore[94], P. Pasuwan[45a,45b], S. Pataraia[100], J. R. Pater[101], A. Pathak[181,j], T. Pauly[36], B. Pearson[115], M. Pedersen[134], L. Pedraza Diaz[119], R. Pedro[140a], T. Peiffer[53], S. V. Peleganchuk[122a,122b], O. Penc[141], H. Peng[60a], B. S. Peralva[81a], M. M. Perego[65], A. P. Pereira Peixoto[140a], D. V. Perepelitsa[29], F. Peri[19], L. Perini[69a,69b], H. Pernegger[36], S. Perrella[70a,70b], K. Peters[46], R. F. Y. Peters[101], B. A. Petersen[36], T. C. Petersen[40], E. Petit[102], A. Petridis[1], C. Petridou[162], P. Petroff[65], M. Petrov[135], F. Petrucci[75a,75b], M. Pettee[183], N. E. Pettersson[103], K. Petukhova[143], A. Peyaud[145], R. Pezoa[147d], L. Pezzotti[71a,71b], T. Pham[105], F. H. Phillips[107], P. W. Phillips[144], M. W. Phipps[173], G. Piacquadio[155], E. Pianori[18], A. Picazio[103], R. H. Pickles[101], R. Piegaia[30], D. Pietreanu[27b], J. E. Pilcher[37], A. D. Pilkington[101], M. Pinamonti[74a,74b], J. L. Pinfold[3], M. Pitt[161], L. Pizzimento[74a,74b], M. -A. Pleier[29], V. Pleskot[143], E. Plotnikova[80], P. Podberezko[122a,122b], R. Poettgen[97], R. Poggi[54], L. Poggioli[65], I. Pogrebnyak[107], D. Pohl[24], I. Pokharel[53], G. Polesello[71a], A. Poley[18], A. Policicchio[73a,73b], R. Polifka[143], A. Polini[23b], C. S. Pollard[46], V. Polychronakos[29], D. Ponomarenko[112], L. Pontecorvo[36], S. Popa[27a], G. A. Popeneciu[27d], L. Portales[5], D. M. Portillo Quintero[58], S. Pospisil[142], K. Potamianos[46], I. N. Potrap[80], C. J. Potter[32], H. Potti[11], T. Poulsen[97], J. Poveda[36], T. D. Powell[149], G. Pownall[46], M. E. Pozo Astigarraga[36], P. Pralavorio[102], S. Prell[79], D. Price[101], M. Primavera[68a], S. Prince[104], M. L. Proffitt[148], N. Proklova[112], K. Prokofiev[63c], F. Prokoshin[80], S. Protopopescu[29], J. Proudfoot[6], M. Przybycien[84a], D. Pudzha[138], A. Puri[173], P. Puzo[65], J. Qian[106], Y. Qin[101], A. Quadt[53], M. Queitsch-Maitland[46], A. Qureshi[1], M. Racko[28a], P. Rados[105], F. Ragusa[69a,69b], G. Rahal[98], J. A. Raine[54], S. Rajagopalan[29], A. Ramirez Morales[93], K. Ran[15a,15d], T. Rashid[65], S. Raspopov[5], D. M. Rauch[46], F. Rauscher[114], S. Rave[100], B. Ravina[149], I. Ravinovich[180], J. H. Rawling[101], M. Raymond[36], A. L. Read[134], N. P. Readioff[58], M. Reale[68a,68b], D. M. Rebuzzi[71a,71b], A. Redelbach[177], G. Redlinger[29], K. Reeves[43], L. Rehnisch[19], J. Reichert[137], D. Reikher[161], A. Reiss[100], A. Rej[151], C. Rembser[36], M. Renda[27b], M. Rescigno[73a], S. Resconi[69a], E. D. Resseguie[137], S. Rettie[175], E. Reynolds[21], O. L. Rezanova[122a,122b], P. Reznicek[143], E. Ricci[76a,76b], R. Richter[115], S. Richter[46], E. Richter-Was[84b], O. Ricken[24], M. Ridel[136], P. Rieck[115], C. J. Riegel[182], O. Rifki[46], M. Rijssenbeek[155], A. Rimoldi[71a,71b], M. Rimoldi[46], L. Rinaldi[23b], G. Ripellino[154], I. Riu[14], J. C. Rivera Vergara[176], F. Rizatdinova[130], E. Rizvi[93], C. Rizzi[36], R. T. Roberts[101], S. H. Robertson[104,af], M. Robin[46], D. Robinson[32], J. E. M. Robinson[46],

C. M. Robles Gajardo[147d], A. Robson[57], A. Rocchi[74a,74b], E. Rocco[100], C. Roda[72a,72b], S. Rodriguez Bosca[174], A. Rodriguez Perez[14], D. Rodriguez Rodriguez[174], A. M. Rodríguez Vera[168b], S. Roe[36], O. Røhne[134], R. Röhrig[115], C. P. A. Roland[66], J. Roloff[59], A. Romaniouk[112], M. Romano[23a,23b], N. Rompotis[91], M. Ronzani[125], L. Roos[136], S. Rosati[73a], K. Rosbach[52], G. Rosin[103], B. J. Rosser[137], E. Rossi[46], E. Rossi[75a,75b], E. Rossi[70a,70b], L. P. Rossi[55b], L. Rossini[69a,69b], R. Rosten[14], M. Rotaru[27b], J. Rothberg[148], D. Rousseau[65], G. Rovelli[71a,71b], A. Roy[11], D. Roy[33e], A. Rozanov[102], Y. Rozen[160], X. Ruan[33e], F. Rubbo[153], F. Rühr[52], A. Ruiz-Martinez[174], A. Rummler[36], Z. Rurikova[52], N. A. Rusakovich[80], H. L. Russell[104], L. Rustige[38,47], J. P. Rutherfoord[7], E. M. Rüttinger[149], M. Rybar[39], G. Rybkin[65], E. B. Rye[134], A. Ryzhov[123], G. F. Rzehorz[53], P. Sabatini[53], G. Sabato[120], S. Sacerdoti[65], H. F -W. Sadrozinski[146], R. Sadykov[80], F. Safai Tehrani[73a], B. Safarzadeh Samani[156], P. Saha[121], S. Saha[104], M. Sahinsoy[61a], A. Sahu[182], M. Saimpert[46], M. Saito[163], T. Saito[163], H. Sakamoto[163], A. Sakharov[125,ao], D. Salamani[54], G. Salamanna[75a,75b], J. E. Salazar Loyola[147d], P. H. Sales De Bruin[172], A. Salnikov[153], J. Salt[174], D. Salvatore[41a,41b], F. Salvatore[156], A. Salvucci[63a,63b,63c], A. Salzburger[36], J. Samarati[36], D. Sammel[52], D. Sampsonidis[162], D. Sampsonidou[162], J. Sánchez[174], A. Sanchez Pineda[67a,67c], H. Sandaker[134], C. O. Sander[46], I. G. Sanderswood[90], M. Sandhoff[182], C. Sandoval[22a], D. P. C. Sankey[144], M. Sannino[55a,55b], Y. Sano[117], A. Sansoni[51], C. Santoni[38], H. Santos[140a,140b], S. N. Santpur[18], A. Santra[174], A. Sapronov[80], J. G. Saraiva[140a,140d], O. Sasaki[82], K. Sato[169], F. Sauerburger[52], E. Sauvan[5], P. Savard[167,ax], N. Savic[115], R. Sawada[163], C. Sawyer[144], L. Sawyer[96,am], C. Sbarra[23b], A. Sbrizzi[23a], T. Scanlon[95], J. Schaarschmidt[148], P. Schacht[115], B. M. Schachtner[114], D. Schaefer[37], L. Schaefer[137], J. Schaeffer[100], S. Schaepe[36], U. Schäfer[100], A. C. Schaffer[65], D. Schaile[114], R. D. Schamberger[155], N. Scharmberg[101], V. A. Schegelsky[138], D. Scheirich[143], F. Schenck[19], M. Schernau[171], C. Schiavi[55a,55b], S. Schier[146], L. K. Schildgen[24], Z. M. Schillaci[26], E. J. Schioppa[36], M. Schioppa[41a,41b], K. E. Schleicher[52], S. Schlenker[36], K. R. Schmidt-Sommerfeld[115], K. Schmieden[36], C. Schmitt[100], S. Schmitt[46], S. Schmitz[100], J. C. Schmoeckel[46], U. Schnoor[52], L. Schoeffel[145], A. Schoening[61b], P. G. Scholer[52], E. Schopf[135], M. Schott[100], J. F. P. Schouwenberg[119], J. Schovancova[36], S. Schramm[54], F. Schroeder[182], A. Schulte[100], H -C. Schultz-Coulon[61a], M. Schumacher[52], B. A. Schumm[146], Ph. Schune[145], A. Schwartzman[153], T. A. Schwarz[106], Ph. Schwemling[145], R. Schwienhorst[107], A. Sciandra[146], G. Sciolla[26], M. Scodeggio[46], M. Scornajenghi[41a,41b], F. Scuri[72a], F. Scutti[105], L. M. Scyboz[115], C. D. Sebastiani[73a,73b], P. Seema[19], S. C. Seidel[118], A. Seiden[146], B. D. Seidlitz[29], T. Seiss[37], J. M. Seixas[81b], G. Sekhniaidze[70a], K. Sekhon[106], S. J. Sekula[42], N. Semprini-Cesari[23a,23b], S. Sen[49], S. Senkin[38], C. Serfon[77], L. Serin[65], L. Serkin[67a,67b], M. Sessa[60a], H. Severini[129], T. Šfiligoj[92], F. Sforza[55a,55b], A. Sfyrla[54], E. Shabalina[53], J. D. Shahinian[146], N. W. Shaikh[45a,45b], D. Shaked Renous[180], L. Y. Shan[15a], R. Shang[173], J. T. Shank[25], M. Shapiro[18], A. Sharma[135], A. S. Sharma[1], P. B. Shatalov[124], K. Shaw[156], S. M. Shaw[101], A. Shcherbakova[138], M. Shehade[180], Y. Shen[129], N. Sherafati[34], A. D. Sherman[25], P. Sherwood[95], L. Shi[158,au], S. Shimizu[82], C. O. Shimmin[183], Y. Shimogama[179], M. Shimojima[116], I. P. J. Shipsey[135], S. Shirabe[88], M. Shiyakova[80,ad], J. Shlomi[180], A. Shmeleva[111], M. J. Shochet[37], J. Shojaii[105], D. R. Shope[129], S. Shrestha[127], E. M. Shrif[33e], E. Shulga[180], P. Sicho[141], A. M. Sickles[173], P. E. Sidebo[154], E. Sideras Haddad[33e], O. Sidiropoulou[36], A. Sidoti[23a,23b], F. Siegert[48], Dj. Sijacki[16], M. Jr. Silva[181], M. V. Silva Oliveira[81a], S. B. Silverstein[45a], S. Simion[65], E. Simioni[100], R. Simoniello[100], S. Simsek[12b], P. Sinervo[167], V. Sinetckii[111,113], N. B. Sinev[132], M. Sioli[23a,23b], I. Siral[106], S. Yu. Sivoklokov[113], J. Sjölin[45a,45b], E. Skorda[97], P. Skubic[129], M. Slawinska[85], K. Sliwa[170], R. Slovak[143], V. Smakhtin[180], B. H. Smart[144], J. Smiesko[28a], N. Smirnov[112], S. Yu. Smirnov[112], Y. Smirnov[112], L. N. Smirnova[113,v], O. Smirnova[97], J. W. Smith[53], M. Smizanska[90], K. Smolek[142], A. Smykiewicz[85], A. A. Snesarev[111], H. L. Snoek[120], I. M. Snyder[132], S. Snyder[29], R. Sobie[176,af], A. Soffer[161], A. Søgaard[50], F. Sohns[53], C. A. Solans Sanchez[36], E. Yu. Soldatov[112], U. Soldevila[174], A. A. Solodkov[123], A. Soloshenko[80], O. V. Solovyanov[123], V. Solovyev[138], P. Sommer[149], H. Son[170], W. Song[144], W. Y. Song[168b], A. Sopczak[142], F. Sopkova[28b], C. L. Sotiropoulou[72a,72b], S. Sottocornola[71a,71b], R. Soualah[67a,67c,g], A. M. Soukharev[122a,122b], D. South[46], S. Spagnolo[68a,68b], M. Spalla[115], M. Spangenberg[178], F. Spanò[94], D. Sperlich[52], T. M. Spieker[61a], R. Spighi[23b], G. Spigo[36], M. Spina[156], D. P. Spiteri[57], M. Spousta[143], A. Stabile[69a,69b], B. L. Stamas[121], R. Stamen[61a], M. Stamenkovic[120], E. Stanecka[85], B. Stanislaus[135], M. M. Stanitzki[46], M. Stankaityte[135], B. Stapf[120], E. A. Starchenko[123], G. H. Stark[146], J. Stark[58], S. H. Stark[40], P. Staroba[141], P. Starovoitov[61a], S. Stärz[104], R. Staszewski[85], G. Stavropoulos[44], M. Stegler[46], P. Steinberg[29], A. L. Steinhebel[132], B. Stelzer[152], H. J. Stelzer[139], O. Stelzer-Chilton[168a], H. Stenzel[56], T. J. Stevenson[156], G. A. Stewart[36], M. C. Stockton[36], G. Stoicea[27b], M. Stolarski[140a], S. Stonjek[115], A. Straessner[48], J. Strandberg[154], S. Strandberg[45a,45b], M. Strauss[129], P. Strizenec[28b], R. Ströhmer[177], D. M. Strom[132], R. Stroynowski[42], A. Strubig[50], S. A. Stucci[29], B. Stugu[17], J. Stupak[129], N. A. Styles[46], D. Su[153], S. Suchek[61a], V. V. Sulin[111], M. J. Sullivan[91], D. M. S. Sultan[54], S. Sultansoy[4c], T. Sumida[86], S. Sun[106], X. Sun[3], K. Suruliz[156], C. J. E. Suster[157], M. R. Sutton[156], S. Suzuki[82], M. Svatos[141], M. Swiatlowski[37], S. P. Swift[2], T. Swirski[177], A. Sydorenko[100], I. Sykora[28a], M. Sykora[143], T. Sykora[143], D. Ta[100], K. Tackmann[46,ab], J. Taenzer[161], A. Taffard[171], R. Tafirout[168a], H. Takai[29], R. Takashima[87], K. Takeda[83], T. Takeshita[150], E. P. Takeva[50], Y. Takubo[82], M. Talby[102],

A. A. Talyshev[122a,122b], N. M. Tamir[161], J. Tanaka[163], M. Tanaka[165], R. Tanaka[65], S. Tapia Araya[173], S. Tapprogge[100], A. Tarek Abouelfadl Mohamed[136], S. Tarem[160], G. Tarna[27b,c], G. F. Tartarelli[69a], P. Tas[143], M. Tasevsky[141], T. Tashiro[86], E. Tassi[41a,41b], A. Tavares Delgado[140a,140b], Y. Tayalati[35e], A. J. Taylor[50], G. N. Taylor[105], W. Taylor[168b], A. S. Tee[90], R. Teixeira De Lima[153], P. Teixeira-Dias[94], H. Ten Kate[36], J. J. Teoh[120], S. Terada[82], K. Terashi[163], J. Terron[99], S. Terzo[14], M. Testa[51], R. J. Teuscher[167,af], S. J. Thais[183], T. Theveneaux-Pelzer[46], F. Thiele[40], D. W. Thomas[94], J. O. Thomas[42], J. P. Thomas[21], A. S. Thompson[57], P. D. Thompson[21], L. A. Thomsen[183], E. Thomson[137], E. J. Thorpe[93], Y. Tian[39], R. E. Ticse Torres[53], V. O. Tikhomirov[111,aq], Yu. A. Tikhonov[122a,122b], S. Timoshenko[112], P. Tipton[183], S. Tisserant[102], K. Todome[23a,23b], S. Todorova-Nova[5], S. Todt[48], J. Tojo[88], S. Tokár[28a], K. Tokushuku[82], E. Tolley[127], K. G. Tomiwa[33e], M. Tomoto[117], L. Tompkins[153,q], B. Tong[59], P. Tornambe[103], E. Torrence[132], H. Torres[48], E. Torró Pastor[148], C. Tosciri[135], J. Toth[102,ae], D. R. Tovey[149], A. Traeet[17], C. J. Treado[125], T. Trefzger[177], F. Tresoldi[156], A. Tricoli[29], I. M. Trigger[168a], S. Trincaz-Duvoid[136], W. Trischuk[167], B. Trocmé[58], A. Trofymov[145], C. Troncon[69a], M. Trovatelli[176], F. Trovato[156], L. Truong[33c], M. Trzebinski[85], A. Trzupek[85], F. Tsai[46], J. C -L. Tseng[135], P. V. Tsiareshka[108,al], A. Tsirigotis[162], N. Tsirintanis[9], V. Tsiskaridze[155], E. G. Tskhadadze[159a], M. Tsopoulou[162], I. I. Tsukerman[124], V. Tsulaia[18], S. Tsuno[82], D. Tsybychev[155], Y. Tu[63b], A. Tudorache[27b], V. Tudorache[27b], T. T. Tulbure[27a], A. N. Tuna[59], S. Turchikhin[80], D. Turgeman[180], I. Turk Cakir[4b,w], R. J. Turner[21], R. T. Turra[69a], P. M. Tuts[39], S. Tzamarias[162], E. Tzovara[100], G. Ucchielli[47], K. Uchida[163], I. Ueda[82], M. Ughetto[45a,45b], F. Ukegawa[169], G. Unal[36], A. Undrus[29], G. Unel[171], F. C. Ungaro[105], Y. Unno[82], K. Uno[163], J. Urban[28b], P. Urquijo[105], G. Usai[8], Z. Uysal[12d], L. Vacavant[102], V. Vacek[142], B. Vachon[104], K. O. H. Vadla[134], A. Vaidya[95], C. Valderanis[114], E. Valdes Santurio[45a,45b], M. Valente[54], S. Valentinetti[23a,23b], A. Valero[174], L. Valéry[46], R. A. Vallance[21], A. Vallier[36], J. A. Valls Ferrer[174], T. R. Van Daalen[14], P. Van Gemmeren[6], I. Van Vulpen[120], M. Vanadia[74a,74b], W. Vandelli[36], A. Vaniachine[166], D. Vannicola[73a,73b], R. Vari[73a], E. W. Varnes[7], C. Varni[55a,55b], T. Varol[42], D. Varouchas[65], K. E. Varvell[157], M. E. Vasile[27b], G. A. Vasquez[176], J. G. Vasquez[183], F. Vazeille[38], D. Vazquez Furelos[14], T. Vazquez Schroeder[36], J. Veatch[53], V. Vecchio[75a,75b], M. J. Veen[120], L. M. Veloce[167], F. Veloso[140a,140c], S. Veneziano[73a], A. Ventura[68a,68b], N. Venturi[36], A. Verbytskyi[115], V. Vercesi[71a], M. Verducci[72a,72b], C. M. Vergel Infante[79], C. Vergis[24], W. Verkerke[120], A. T. Vermeulen[120], J. C. Vermeulen[120], M. C. Vetterli[152,ax], N. Viaux Maira[147d], M. Vicente Barreto Pinto[54], T. Vickey[149], O. E. Vickey Boeriu[149], G. H. A. Viehhauser[135], L. Vigani[61b], M. Villa[23a,23b], M. Villaplana Perez[69a,69b], E. Vilucchi[51], M. G. Vincter[34], V. B. Vinogradov[80], G. S. Virdee[21], A. Vishwakarma[46], C. Vittori[23a,23b], I. Vivarelli[156], M. Vogel[182], P. Vokac[142], S. E. von Buddenbrock[33e], E. Von Toerne[24], V. Vorobel[143], K. Vorobev[112], M. Vos[174], J. H. Vossebeld[91], M. Vozak[101], N. Vranjes[16], M. Vranjes Milosavljevic[16], V. Vrba[142], M. Vreeswijk[120], R. Vuillermet[36], I. Vukotic[37], P. Wagner[24], W. Wagner[182], J. Wagner-Kuhr[114], S. Wahdan[182], H. Wahlberg[89], V. M. Walbrecht[115], J. Walder[90], R. Walker[114], S. D. Walker[94], W. Walkowiak[151], V. Wallangen[45a,45b], A. M. Wang[59], C. Wang[60c], C. Wang[60b], F. Wang[181], H. Wang[18], H. Wang[3], J. Wang[157], J. Wang[61b], P. Wang[42], Q. Wang[129], R. -J. Wang[100], R. Wang[60a], R. Wang[6], S. M. Wang[158], W. T. Wang[60a], W. Wang[15c,ag], W. X. Wang[60a,ag], Y. Wang[60a,an], Z. Wang[60c], C. Wanotayaroj[46], A. Warburton[104], C. P. Ward[32], D. R. Wardrope[95], N. Warrack[57], A. Washbrook[50], A. T. Watson[21], M. F. Watson[21], G. Watts[148], B. M. Waugh[95], A. F. Webb[11], S. Webb[100], C. Weber[183], M. S. Weber[20], S. A. Weber[34], S. M. Weber[61a], A. R. Weidberg[135], J. Weingarten[47], M. Weirich[100], C. Weiser[52], P. S. Wells[36], T. Wenaus[29], T. Wengler[36], S. Wenig[36], N. Wermes[24], M. D. Werner[79], M. Wessels[61a], T. D. Weston[20], K. Whalen[132], N. L. Whallon[148], A. M. Wharton[90], A. S. White[106], A. White[8], M. J. White[1], D. Whiteson[171], B. W. Whitmore[90], W. Wiedenmann[181], M. Wielers[144], N. Wieseotte[100], C. Wiglesworth[40], L. A. M. Wiik-Fuchs[52], F. Wilk[101], H. G. Wilkens[36], L. J. Wilkins[94], H. H. Williams[137], S. Williams[32], C. Willis[107], S. Willocq[103], J. A. Wilson[21], I. Wingerter-Seez[5], E. Winkels[156], F. Winklmeier[132], O. J. Winston[156], B. T. Winter[52], M. Wittgen[153], M. Wobisch[96], A. Wolf[100], T. M. H. Wolf[120], R. Wolff[102], R. Wölker[135], J. Wollrath[52], M. W. Wolter[85], H. Wolters[140a,140c], V. W. S. Wong[175], N. L. Woods[146], S. D. Worm[21], B. K. Wosiek[85], K. W. Woźniak[85], K. Wraight[57], S. L. Wu[181], X. Wu[54], Y. Wu[60a], T. R. Wyatt[101], B. M. Wynne[50], S. Xella[40], Z. Xi[106], L. Xia[178], X. Xiao[106], D. Xu[15a], H. Xu[60a,c], L. Xu[29], T. Xu[145], W. Xu[106], Z. Xu[60b], Z. Xu[153], B. Yabsley[157], S. Yacoob[33a], K. Yajima[133], D. P. Yallup[95], D. Yamaguchi[165], Y. Yamaguchi[165], A. Yamamoto[82], M. Yamatani[163], T. Yamazaki[163], Y. Yamazaki[83], Z. Yan[25], H. J. Yang[60c,60d], H. T. Yang[18], S. Yang[78], X. Yang[58,60b], Y. Yang[163], W -M. Yao[18], Y. C. Yap[46], Y. Yasu[82], E. Yatsenko[60c,60d], J. Ye[42], S. Ye[29], I. Yeletskikh[80], M. R. Yexley[90], E. Yigitbasi[25], K. Yorita[179], K. Yoshihara[137], C. J. S. Young[36], C. Young[153], J. Yu[79], R. Yuan[60b,i], X. Yue[61a], S. P. Y. Yuen[24], B. Zabinski[85], G. Zacharis[10], E. Zaffaroni[54], J. Zahreddine[136], A. M. Zaitsev[123,ap], T. Zakareishvili[159b], N. Zakharchuk[34], S. Zambito[59], D. Zanzi[36], D. R. Zaripovas[57], S. V. Zeißner[47], C. Zeitnitz[182], G. Zemaityte[135], J. C. Zeng[173], O. Zenin[123], T. Ženiš[28a], D. Zerwas[65], M. Zgubič[135], D. F. Zhang[15b], F. Zhang[181], G. Zhang[15b], H. Zhang[15c], J. Zhang[6], L. Zhang[15c], L. Zhang[60a], M. Zhang[173], R. Zhang[24], X. Zhang[60b], Y. Zhang[15a,15d], Z. Zhang[63a], Z. Zhang[65], P. Zhao[49], Y. Zhao[60b], Z. Zhao[60a], A. Zhemchugov[80], Z. Zheng[106], D. Zhong[173], B. Zhou[106], C. Zhou[181], M. S. Zhou[15a,15d], M. Zhou[155], N. Zhou[60c], Y. Zhou[7], C. G. Zhu[60b], H. L. Zhu[60a],

H. Zhu[15a], J. Zhu[106], Y. Zhu[60a], X. Zhuang[15a], K. Zhukov[111], V. Zhulanov[122a,122b], D. Zieminska[66], N. I. Zimine[80], S. Zimmermann[52], Z. Zinonos[115], M. Ziolkowski[151], L. Živković[16], G. Zobernig[181], A. Zoccoli[23a,23b], K. Zoch[53], T. G. Zorbas[149], R. Zou[37], L. Zwalinski[36]

[1] Department of Physics, University of Adelaide, Adelaide, Australia
[2] Physics Department, SUNY Albany, Albany, NY, USA
[3] Department of Physics, University of Alberta, Edmonton, AB, Canada
[4] [(a)]Department of Physics, Ankara University, Ankara, Turkey; [(b)]Istanbul Aydin University, Istanbul, Turkey; [(c)]Division of Physics, TOBB University of Economics and Technology, Ankara, Turkey
[5] LAPP, Université Grenoble Alpes, Université Savoie Mont Blanc, CNRS/IN2P3, Annecy, France
[6] High Energy Physics Division, Argonne National Laboratory, Argonne, IL, USA
[7] Department of Physics, University of Arizona, Tucson, AZ, USA
[8] Department of Physics, University of Texas at Arlington, Arlington, TX, USA
[9] Physics Department, National and Kapodistrian University of Athens, Athens, Greece
[10] Physics Department, National Technical University of Athens, Zografou, Greece
[11] Department of Physics, University of Texas at Austin, Austin, TX, USA
[12] [(a)]Bahcesehir University, Faculty of Engineering and Natural Sciences, Istanbul, Turkey; [(b)]Istanbul Bilgi University, Faculty of Engineering and Natural Sciences, Istanbul, Turkey; [(c)]Department of Physics, Bogazici University, Istanbul, Turkey; [(d)]Department of Physics Engineering, Gaziantep University, Gaziantep, Turkey
[13] Institute of Physics, Azerbaijan Academy of Sciences, Baku, Azerbaijan
[14] Institut de Física d'Altes Energies (IFAE), Barcelona Institute of Science and Technology, Barcelona, Spain
[15] [(a)]Institute of High Energy Physics, Chinese Academy of Sciences, Beijing, China; [(b)]Physics Department, Tsinghua University, Beijing, China; [(c)]Department of Physics, Nanjing University, Nanjing, China; [(d)]University of Chinese Academy of Science (UCAS), Beijing, China
[16] Institute of Physics, University of Belgrade, Belgrade, Serbia
[17] Department for Physics and Technology, University of Bergen, Bergen, Norway
[18] Physics Division, Lawrence Berkeley National Laboratory and University of California, Berkeley, CA, USA
[19] Institut für Physik, Humboldt Universität zu Berlin, Berlin, Germany
[20] Albert Einstein Center for Fundamental Physics and Laboratory for High Energy Physics, University of Bern, Bern, Switzerland
[21] School of Physics and Astronomy, University of Birmingham, Birmingham, UK
[22] [(a)]Facultad de Ciencias y Centro de Investigaciónes, Universidad Antonio Nariño, Bogotá, Colombia; [(b)]Departamento de Física, Universidad Nacional de Colombia, Bogotá, Colombia
[23] [(a)]Dipartimento di Fisica, INFN Bologna and Universita' di Bologna, Bologna, Italy; [(b)]INFN Sezione di Bologna, Bologna, Italy
[24] Physikalisches Institut, Universität Bonn, Bonn, Germany
[25] Department of Physics, Boston University, Boston, MA, USA
[26] Department of Physics, Brandeis University, Waltham, MA, USA
[27] [(a)]Transilvania University of Brasov, Brasov, Romania; [(b)]Horia Hulubei National Institute of Physics and Nuclear Engineering, Bucharest, Romania; [(c)]Department of Physics, Alexandru Ioan Cuza University of Iasi, Iasi, Romania; [(d)]National Institute for Research and Development of Isotopic and Molecular Technologies, Physics Department, Cluj-Napoca, Romania; [(e)]University Politehnica Bucharest, Bucharest, Romania; [(f)]West University in Timisoara, Timisoara, Romania
[28] [(a)]Faculty of Mathematics, Physics and Informatics, Comenius University, Bratislava, Slovakia; [(b)]Department of Subnuclear Physics, Institute of Experimental Physics of the Slovak Academy of Sciences, Kosice, Slovak Republic
[29] Physics Department, Brookhaven National Laboratory, Upton, NY, USA
[30] Departamento de Física, Universidad de Buenos Aires, Buenos Aires, Argentina
[31] California State University, Long Beach, CA, USA
[32] Cavendish Laboratory, University of Cambridge, Cambridge, UK
[33] [(a)]Department of Physics, University of Cape Town, Cape Town, South Africa; [(b)]iThemba Labs, Western Cape, South Africa; [(c)]Department of Mechanical Engineering Science, University of Johannesburg, Johannesburg, South Africa; [(d)]University of South Africa, Department of Physics, Pretoria, South Africa; [(e)]School of Physics, University of the Witwatersrand, Johannesburg, South Africa

[34] Department of Physics, Carleton University, Ottawa, ON, Canada
[35] [(a)]Faculté des Sciences Ain Chock, Réseau Universitaire de Physique des Hautes Energies, Université Hassan II, Casablanca, Morocco; [(b)]Faculté des Sciences, Université Ibn-Tofail, Kénitra, Morocco; [(c)]Faculté des Sciences Semlalia, Université Cadi Ayyad, LPHEA-Marrakech, Marrakesh, Morocco; [(d)]Faculté des Sciences, Université Mohamed Premier and LPTPM, Oujda, Morocco; [(e)]Faculté des sciences, Université Mohammed V, Rabat, Morocco
[36] CERN, Geneva, Switzerland
[37] Enrico Fermi Institute, University of Chicago, Chicago, IL, USA
[38] LPC, Université Clermont Auvergne, CNRS/IN2P3, Clermont-Ferrand, France
[39] Nevis Laboratory, Columbia University, Irvington, NY, USA
[40] Niels Bohr Institute, University of Copenhagen, Copenhagen, Denmark
[41] [(a)]Dipartimento di Fisica, Università della Calabria, Rende, Italy; [(b)]INFN Gruppo Collegato di Cosenza, Laboratori Nazionali di Frascati, Frascati, Italy
[42] Physics Department, Southern Methodist University, Dallas, TX, USA
[43] Physics Department, University of Texas at Dallas, Richardson, TX, USA
[44] National Centre for Scientific Research "Demokritos", Agia Paraskevi, Greece
[45] [(a)]Department of Physics, Stockholm University, Stockholm, Sweden; [(b)]Oskar Klein Centre, Stockholm, Sweden
[46] Deutsches Elektronen-Synchrotron DESY, Hamburg and Zeuthen, Germany
[47] Lehrstuhl für Experimentelle Physik IV, Technische Universität Dortmund, Dortmund, Germany
[48] Institut für Kern- und Teilchenphysik, Technische Universität Dresden, Dresden, Germany
[49] Department of Physics, Duke University, Durham, NC, USA
[50] SUPA-School of Physics and Astronomy, University of Edinburgh, Edinburgh, UK
[51] INFN e Laboratori Nazionali di Frascati, Frascati, Italy
[52] Physikalisches Institut, Albert-Ludwigs-Universität Freiburg, Freiburg, Germany
[53] II. Physikalisches Institut, Georg-August-Universität Göttingen, Göttingen, Germany
[54] Département de Physique Nucléaire et Corpusculaire, Université de Genève, Geneva, Switzerland
[55] [(a)]Dipartimento di Fisica, Università di Genova, Genoa, Italy; [(b)]INFN Sezione di Genova, Genoa, Italy
[56] II. Physikalisches Institut, Justus-Liebig-Universität Giessen, Giessen, Germany
[57] SUPA-School of Physics and Astronomy, University of Glasgow, Glasgow, UK
[58] LPSC, Université Grenoble Alpes, CNRS/IN2P3, Grenoble INP, Grenoble, France
[59] Laboratory for Particle Physics and Cosmology, Harvard University, Cambridge, MA, USA
[60] [(a)]Department of Modern Physics and State Key Laboratory of Particle Detection and Electronics, University of Science and Technology of China, Hefei, China; [(b)]Institute of Frontier and Interdisciplinary Science and Key Laboratory of Particle Physics and Particle Irradiation (MOE), Shandong University, Qingdao, China; [(c)]School of Physics and Astronomy, Shanghai Jiao Tong University, KLPPAC-MoE, SKLPPC, Shanghai, China; [(d)]Tsung-Dao Lee Institute, Shanghai, China
[61] [(a)]Kirchhoff-Institut für Physik, Ruprecht-Karls-Universität Heidelberg, Heidelberg, Germany; [(b)]Physikalisches Institut, Ruprecht-Karls-Universität Heidelberg, Heidelberg, Germany
[62] Faculty of Applied Information Science, Hiroshima Institute of Technology, Hiroshima, Japan
[63] [(a)]Department of Physics, Chinese University of Hong Kong, Shatin, N.T., Hong Kong; [(b)]Department of Physics, University of Hong Kong, Pok Fu Lam, Hong Kong; [(c)]Department of Physics and Institute for Advanced Study, Hong Kong University of Science and Technology, Clear Water Bay, Kowloon, Hong Kong, China
[64] Department of Physics, National Tsing Hua University, Hsinchu, Taiwan
[65] IJCLab, Université Paris-Saclay, CNRS/IN2P3, 91405 Orsay, France
[66] Department of Physics, Indiana University, Bloomington, IN, USA
[67] [(a)]INFN Gruppo Collegato di Udine, Sezione di Trieste, Udine, Italy; [(b)]ICTP, Trieste, Italy; [(c)]Dipartimento Politecnico di Ingegneria e Architettura, Università di Udine, Udine, Italy
[68] [(a)]INFN Sezione di Lecce, Lecce, Italy; [(b)]Dipartimento di Matematica e Fisica, Università del Salento, Lecce, Italy
[69] [(a)]INFN Sezione di Milano, Milan, Italy; [(b)]Dipartimento di Fisica, Università di Milano, Milan, Italy
[70] [(a)]INFN Sezione di Napoli, Naples, Italy; [(b)]Dipartimento di Fisica, Università di Napoli, Naples, Italy
[71] [(a)]INFN Sezione di Pavia, Pavia, Italy; [(b)]Dipartimento di Fisica, Università di Pavia, Pavia, Italy
[72] [(a)]INFN Sezione di Pisa, Pisa, Italy; [(b)]Dipartimento di Fisica E. Fermi, Università di Pisa, Pisa, Italy
[73] [(a)]INFN Sezione di Roma, Rome, Italy; [(b)]Dipartimento di Fisica, Sapienza Università di Roma, Rome, Italy

[74] [(a)]INFN Sezione di Roma Tor Vergata, Rome, Italy; [(b)]Dipartimento di Fisica, Università di Roma Tor Vergata, Rome, Italy
[75] [(a)]INFN Sezione di Roma Tre, Rome, Italy; [(b)]Dipartimento di Matematica e Fisica, Università Roma Tre, Rome, Italy
[76] [(a)]INFN-TIFPA, Povo, Italy; [(b)]Università degli Studi di Trento, Trento, Italy
[77] Institut für Astro- und Teilchenphysik, Leopold-Franzens-Universität, Innsbruck, Austria
[78] University of Iowa, Iowa City, IA, USA
[79] Department of Physics and Astronomy, Iowa State University, Ames, IA, USA
[80] Joint Institute for Nuclear Research, Dubna, Russia
[81] [(a)]Departamento de Engenharia Elétrica, Universidade Federal de Juiz de Fora (UFJF), Juiz de Fora, Brazil; [(b)]Universidade Federal do Rio De Janeiro COPPE/EE/IF, Rio de Janeiro, Brazil; [(c)]Universidade Federal de São João del Rei (UFSJ), São João del Rei, Brazil; [(d)]Instituto de Física, Universidade de São Paulo, São Paulo, Brazil
[82] KEK, High Energy Accelerator Research Organization, Tsukuba, Japan
[83] Graduate School of Science, Kobe University, Kobe, Japan
[84] [(a)]AGH University of Science and Technology, Faculty of Physics and Applied Computer Science, Kraków, Poland ; [(b)]Marian Smoluchowski Institute of Physics, Jagiellonian University, Kraków, Poland
[85] Institute of Nuclear Physics Polish Academy of Sciences, Kraków, Poland
[86] Faculty of Science, Kyoto University, Kyoto, Japan
[87] Kyoto University of Education, Kyoto, Japan
[88] Research Center for Advanced Particle Physics and Department of Physics, Kyushu University, Fukuoka , Japan
[89] Instituto de Física La Plata, Universidad Nacional de La Plata and CONICET, La Plata, Argentina
[90] Physics Department, Lancaster University, Lancaster, UK
[91] Oliver Lodge Laboratory, University of Liverpool, Liverpool, UK
[92] Department of Experimental Particle Physics, Jožef Stefan Institute and Department of Physics, University of Ljubljana, Ljubljana, Slovenia
[93] School of Physics and Astronomy, Queen Mary University of London, London, UK
[94] Department of Physics, Royal Holloway University of London, Egham, UK
[95] Department of Physics and Astronomy, University College London, London, UK
[96] Louisiana Tech University, Ruston, LA, USA
[97] Fysiska institutionen, Lunds universitet, Lund, Sweden
[98] Centre de Calcul de l'Institut National de Physique Nucléaire et de Physique des Particules (IN2P3), Villeurbanne, France
[99] Departamento de Física Teorica C-15 and CIAFF, Universidad Autónoma de Madrid, Madrid, Spain
[100] Institut für Physik, Universität Mainz, Mainz, Germany
[101] School of Physics and Astronomy, University of Manchester, Manchester, UK
[102] CPPM, Aix-Marseille Université, CNRS/IN2P3, Marseille, France
[103] Department of Physics, University of Massachusetts, Amherst, MA, USA
[104] Department of Physics, McGill University, Montreal, QC, Canada
[105] School of Physics, University of Melbourne, Melbourne, VIC, Australia
[106] Department of Physics, University of Michigan, Ann Arbor, MI, USA
[107] Department of Physics and Astronomy, Michigan State University, East Lansing, MI, USA
[108] B.I. Stepanov Institute of Physics, National Academy of Sciences of Belarus, Minsk, Belarus
[109] Research Institute for Nuclear Problems of Byelorussian State University, Minsk, Belarus
[110] Group of Particle Physics, University of Montreal, Montreal, QC, Canada
[111] P.N. Lebedev Physical Institute of the Russian Academy of Sciences, Moscow, Russia
[112] National Research Nuclear University MEPhI, Moscow, Russia
[113] D.V. Skobeltsyn Institute of Nuclear Physics, M.V. Lomonosov Moscow State University, Moscow, Russia
[114] Fakultät für Physik, Ludwig-Maximilians-Universität München, Munich, Germany
[115] Max-Planck-Institut für Physik (Werner-Heisenberg-Institut), Munich, Germany
[116] Nagasaki Institute of Applied Science, Nagasaki, Japan
[117] Graduate School of Science and Kobayashi-Maskawa Institute, Nagoya University, Nagoya, Japan
[118] Department of Physics and Astronomy, University of New Mexico, Albuquerque, NM, USA
[119] Institute for Mathematics, Astrophysics and Particle Physics, Radboud University Nijmegen/Nikhef, Nijmegen, The Netherlands

[120] Nikhef National Institute for Subatomic Physics and University of Amsterdam, Amsterdam, The Netherlands
[121] Department of Physics, Northern Illinois University, DeKalb, IL, USA
[122] [(a)]Budker Institute of Nuclear Physics and NSU, SB RAS, Novosibirsk, Russia; [(b)]Novosibirsk State University, Novosibirsk, Russia
[123] Institute for High Energy Physics of the National Research Centre Kurchatov Institute, Protvino, Russia
[124] Institute for Theoretical and Experimental Physics named by A.I. Alikhanov of National Research Centre "Kurchatov Institute", Moscow, Russia
[125] Department of Physics, New York University, New York, NY, USA
[126] Ochanomizu University, Otsuka, Bunkyo-ku, Tokyo, Japan
[127] Ohio State University, Columbus, OH, USA
[128] Faculty of Science, Okayama University, Okayama, Japan
[129] Homer L. Dodge Department of Physics and Astronomy, University of Oklahoma, Norman, OK, USA
[130] Department of Physics, Oklahoma State University, Stillwater, OK, USA
[131] Palacký University, RCPTM, Joint Laboratory of Optics, Olomouc, Czech Republic
[132] Center for High Energy Physics, University of Oregon, Eugene, OR, USA
[133] Graduate School of Science, Osaka University, Osaka, Japan
[134] Department of Physics, University of Oslo, Oslo, Norway
[135] Department of Physics, Oxford University, Oxford, UK
[136] LPNHE, Sorbonne Université, Université de Paris, CNRS/IN2P3, Paris, France
[137] Department of Physics, University of Pennsylvania, Philadelphia, PA, USA
[138] Konstantinov Nuclear Physics Institute of National Research Centre "Kurchatov Institute", PNPI, St. Petersburg, Russia
[139] Department of Physics and Astronomy, University of Pittsburgh, Pittsburgh, PA, USA
[140] [(a)]Laboratório de Instrumentação e Física Experimental de Partículas - LIP, Lisbon, Portugal; [(b)]Departamento de Física, Faculdade de Ciências, Universidade de Lisboa, Lisbon, Portugal; [(c)]Departamento de Física, Universidade de Coimbra, Coimbra, Portugal; [(d)]Centro de Física Nuclear da Universidade de Lisboa, Lisbon, Portugal; [(e)]Departamento de Física, Universidade do Minho, Braga, Portugal; [(f)]Departamento de Física Teórica y del Cosmos, Universidad de Granada, Granada, Spain; [(g)]Dep Física and CEFITEC of Faculdade de Ciências e Tecnologia, Universidade Nova de Lisboa, Caparica, Portugal; [(h)]Instituto Superior Técnico, Universidade de Lisboa, Lisbon, Portugal
[141] Institute of Physics of the Czech Academy of Sciences, Prague, Czech Republic
[142] Czech Technical University in Prague, Prague, Czech Republic
[143] Charles University, Faculty of Mathematics and Physics, Prague, Czech Republic
[144] Particle Physics Department, Rutherford Appleton Laboratory, Didcot, UK
[145] IRFU, CEA, Université Paris-Saclay, Gif-sur-Yvette, France
[146] Santa Cruz Institute for Particle Physics, University of California Santa Cruz, Santa Cruz, CA, USA
[147] [(a)]Departamento de Física, Pontificia Universidad Católica de Chile, Santiago, Chile; [(b)]Universidad Andres Bello, Department of Physics, Santiago, Chile; [(c)]Instituto de Alta Investigación, Universidad de Tarapacá, Arica, Chile; [(d)]Departamento de Física, Universidad Técnica Federico Santa María, Valparaíso, Chile
[148] Department of Physics, University of Washington, Seattle, WA, USA
[149] Department of Physics and Astronomy, University of Sheffield, Sheffield, UK
[150] Department of Physics, Shinshu University, Nagano, Japan
[151] Department Physik, Universität Siegen, Siegen, Germany
[152] Department of Physics, Simon Fraser University, Burnaby, BC, Canada
[153] SLAC National Accelerator Laboratory, Stanford, CA, USA
[154] Physics Department, Royal Institute of Technology, Stockholm, Sweden
[155] Departments of Physics and Astronomy, Stony Brook University, Stony Brook, NY, USA
[156] Department of Physics and Astronomy, University of Sussex, Brighton, UK
[157] School of Physics, University of Sydney, Sydney, Australia
[158] Institute of Physics, Academia Sinica, Taipei, Taiwan
[159] [(a)]E. Andronikashvili Institute of Physics, Iv. Javakhishvili Tbilisi State University, Tbilisi, Georgia; [(b)]High Energy Physics Institute, Tbilisi State University, Tbilisi, Georgia
[160] Department of Physics, Technion, Israel Institute of Technology, Haifa, Israel
[161] Raymond and Beverly Sackler School of Physics and Astronomy, Tel Aviv University, Tel Aviv, Israel
[162] Department of Physics, Aristotle University of Thessaloniki, Thessaloniki, Greece

[163] International Center for Elementary Particle Physics and Department of Physics, University of Tokyo, Tokyo, Japan
[164] Graduate School of Science and Technology, Tokyo Metropolitan University, Tokyo, Japan
[165] Department of Physics, Tokyo Institute of Technology, Tokyo, Japan
[166] Tomsk State University, Tomsk, Russia
[167] Department of Physics, University of Toronto, Toronto, ON, Canada
[168] [(a)]TRIUMF, Vancouver, BC, Canada; [(b)]Department of Physics and Astronomy, York University, Toronto, ON, Canada
[169] Division of Physics and Tomonaga Center for the History of the Universe, Faculty of Pure and Applied Sciences, University of Tsukuba, Tsukuba, Japan
[170] Department of Physics and Astronomy, Tufts University, Medford, MA, USA
[171] Department of Physics and Astronomy, University of California Irvine, Irvine, CA, USA
[172] Department of Physics and Astronomy, University of Uppsala, Uppsala, Sweden
[173] Department of Physics, University of Illinois, Urbana, IL, USA
[174] Instituto de Física Corpuscular (IFIC), Centro Mixto Universidad de Valencia-CSIC, Valencia, Spain
[175] Department of Physics, University of British Columbia, Vancouver, BC, Canada
[176] Department of Physics and Astronomy, University of Victoria, Victoria, BC, Canada
[177] Fakultät für Physik und Astronomie, Julius-Maximilians-Universität Würzburg, Würzburg, Germany
[178] Department of Physics, University of Warwick, Coventry, UK
[179] Waseda University, Tokyo, Japan
[180] Department of Particle Physics, Weizmann Institute of Science, Rehovot, Israel
[181] Department of Physics, University of Wisconsin, Madison, WI, USA
[182] Fakultät für Mathematik und Naturwissenschaften, Fachgruppe Physik, Bergische Universität Wuppertal, Wuppertal, Germany
[183] Department of Physics, Yale University, New Haven, CT, USA
[184] Yerevan Physics Institute, Yerevan, Armenia

[a] Also at Borough of Manhattan Community College, City University of New York, New York, NY, USA
[b] Also at CERN, Geneva, Switzerland
[c] Also at CPPM, Aix-Marseille Université, CNRS/IN2P3, Marseille, France
[d] Also at Département de Physique Nucléaire et Corpusculaire, Université de Genève, Geneva, Switzerland
[e] Also at Departament de Fisica de la Universitat Autonoma de Barcelona, Barcelona, Spain
[f] Also at Departamento de Física, Instituto Superior Técnico, Universidade de Lisboa, Lisbon, Portugal
[g] Also at Department of Applied Physics and Astronomy, University of Sharjah, Sharjah, United Arab Emirates
[h] Also at Department of Financial and Management Engineering, University of the Aegean, Chios, Greece
[i] Also at Department of Physics and Astronomy, Michigan State University, East Lansing, MI, USA
[j] Also at Department of Physics and Astronomy, University of Louisville, Louisville, KY, USA
[k] Also at Department of Physics, Ben Gurion University of the Negev, Beer Sheva, Israel
[l] Also at Department of Physics, California State University, East Bay, USA
[m] Also at Department of Physics, California State University, Fresno, USA
[n] Also at Department of Physics, California State University, Sacramento, USA
[o] Also at Department of Physics, King's College London, London, UK
[p] Also at Department of Physics, St. Petersburg State Polytechnical University, St. Petersburg, Russia
[q] Also at Department of Physics, Stanford University, Stanford, CA, USA
[r] Also at Department of Physics, University of Adelaide, Adelaide, Australia
[s] Also at Department of Physics, University of Fribourg, Fribourg, Switzerland
[t] Also at Department of Physics, University of Michigan, Ann Arbor, MI, USA
[u] Also at Dipartimento di Matematica, Informatica e Fisica, Università di Udine, Udine, Italy
[v] Also at Faculty of Physics, M.V. Lomonosov Moscow State University, Moscow, Russia
[w] Also at Giresun University, Faculty of Engineering, Giresun, Turkey
[x] Also at Graduate School of Science, Osaka University, Osaka, Japan
[y] Also at Hellenic Open University, Patras, Greece
[z] Also at IJCLab, Université Paris-Saclay, CNRS/IN2P3, 91405, Orsay, France
[aa] Also at Institucio Catalana de Recerca i Estudis Avancats, ICREA, Barcelona, Spain
[ab] Also at Institut für Experimentalphysik, Universität Hamburg, Hamburg, Germany

[ac] Also at Institute for Mathematics, Astrophysics and Particle Physics, Radboud University Nijmegen/Nikhef, Nijmegen, The Netherlands
[ad] Also at Institute for Nuclear Research and Nuclear Energy (INRNE) of the Bulgarian Academy of Sciences, Sofia, Bulgaria
[ae] Also at Institute for Particle and Nuclear Physics, Wigner Research Centre for Physics, Budapest, Hungary
[af] Also at Institute of Particle Physics (IPP), Vancouver, Canada
[ag] Also at Institute of Physics, Academia Sinica, Taipei, Taiwan
[ah] Also at Institute of Physics, Azerbaijan Academy of Sciences, Baku, Azerbaijan
[ai] Also at Institute of Theoretical Physics, Ilia State University, Tbilisi, Georgia
[aj] Also at Instituto de Fisica Teorica, IFT-UAM/CSIC, Madrid, Spain
[ak] Also at Istanbul University, Dept. of Physics, Istanbul, Turkey
[al] Also at Joint Institute for Nuclear Research, Dubna, Russia
[am] Also at Louisiana Tech University, Ruston, LA, USA
[an] Also at LPNHE, Sorbonne Université, Université de Paris, CNRS/IN2P3, Paris, France
[ao] Also at Manhattan College, New York, NY, USA
[ap] Also at Moscow Institute of Physics and Technology State University, Dolgoprudny, Russia
[aq] Also at National Research Nuclear University MEPhI, Moscow, Russia
[ar] Also at Physics Department, An-Najah National University, Nablus, Palestine
[as] Also at Physics Dept, University of South Africa, Pretoria, South Africa
[at] Also at Physikalisches Institut, Albert-Ludwigs-Universität Freiburg, Freiburg, Germany
[au] Also at School of Physics, Sun Yat-sen University, Guangzhou, China
[av] Also at The City College of New York, New York, NY, USA
[aw] Also at The Collaborative Innovation Center of Quantum Matter (CICQM), Beijing, China
[ax] Also at TRIUMF, Vancouver, BC, Canada
[ay] Also at Universita di Napoli Parthenope, Naples, Italy
* Deceased